



Originally published as:

Güntner, A., Stuck, J., Werth, S., Döll, P., Verzano, K., Merz, B. (2007): A global analysis of temporal and spatial variations in continental water storage. - Water Resources Research (AGU), 43, W05416

DOI: [10.1029/2006WR005247](https://doi.org/10.1029/2006WR005247)

A global analysis of temporal and spatial variations in continental water storage

Andreas Güntner (1), Jochen Stuck (1), Susanna Werth (1), Petra Döll (2), Kerstin Verzano (3), Bruno Merz (1)

(1) GeoForschungsZentrum Potsdam (GFZ), Telegrafenberg, 14473 Potsdam, Germany;
guentner@gfz-potsdam.de

(2) Institute of Physical Geography, University of Frankfurt am Main, P.O. Box 111932,
60054 Frankfurt am Main, Germany.

(3) Centre for Environmental Systems Research, University of Kassel, 34109 Kassel,
Germany

Manuscript accepted by Water Resources Research

08.12.2006

Abstract

While continental water storage plays a key role in the Earth's water, energy and biogeochemical cycles, its temporal and spatial variations are poorly known, in particular for large areas. This study analyzes water storage simulated with the WaterGAP Global Hydrology Model (WGHM). The model represents four major storage compartments: surface water, snow, soil and groundwater. Water storage variations are analyzed for the period 1961-1995 with 0.5° resolution, for the major global climate zones, and for the 30 largest river basins worldwide. Seasonal variations are the dominant storage change signal with maximum values in the marginal tropics and in snow-dominated high-latitude areas. Interannual variations are associated with large-scale oscillations such as ENSO. The contribution of individual water storage compartments to total storage change varies with the climate region and the time scale under consideration. In most regions, a prominent role of storage variations in surface water bodies is found. Surface water reduces markedly the spatial correlation lengths of water storage fields. The simulation results are evaluated against storage variations of combined atmospheric-terrestrial water balance studies and other global models. This study contributes to an improved understanding of continental water storage for which the consistent integration of model results and new observations such as from time-variable gravity data of the GRACE satellite mission is required.

1. Introduction

Continental water storage plays a key role in the Earth's water, energy and biogeochemical cycles. Water storage supplies the evaporative demand of plants and serves for human consumption, including various types of agricultural and industrial use. Total continental water storage is composed of water on vegetation surfaces, in the biomass and in the unsaturated soil or rock zone, of groundwater, snow and ice, and of surface water in rivers, wetlands, natural lakes and man-made reservoirs. The change in continental water storage (ΔS) is a fundamental component of the hydrological cycle. Precipitation reaching the land surface is balanced by evapotranspiration, runoff and storage change. Associated with storage changes, runoff from the continental areas to the ocean is one factor governing sea level variations. In addition, as ΔS involves mass transports and mass redistribution at the Earth's surface and interior, it acts on geophysical phenomena such as temporal variations of the gravity field [Wahr *et al.*, 1998], Earth rotation [e.g., Cazenave *et al.*, 1999] or elastic oscillations of the Earth surface [Bevis *et al.*, 2005].

In spite of the large importance of water storage from local to global scales, temporal and spatial variations of water storage are presently not known with sufficient accuracy for large areas [Rodell and Famiglietti, 1999; Alsdorf *et al.*, 2003]. A main reason is the lack of adequate large-scale monitoring systems. Individual soil moisture or groundwater measurements [e.g., Robock *et al.*, 2000] give only local estimates of water storage. Monitoring from satellites would in principle allow for a large spatial coverage. However, measurements of soil water storage usually are limited to the uppermost soil layer and to areas free of a dense vegetation cover [Wagner *et al.*, 2003]. For surface waters, storage changes can be observed by means of altimetry or radar remote sensing of water levels in rivers, lakes or inundated floodplains [Birkett, 1998; Alsdorf *et al.*, 2000; Birkett *et al.*, 2002; Maheu *et al.*, 2003], but its application is limited to individual targets so far. An outstanding new global data source for ΔS was expected from the GRACE satellite mission [Tapley *et al.*, 2004a], where time-variable gravity fields of the Earth allow to resolve for ΔS after removal of atmospheric, oceanic and other mass variations [Wahr *et al.*, 1998; Dickey *et al.*, 1999; Rodell and Famiglietti, 1999; Swenson *et al.*, 2003]. Results from GRACE observations so far clearly show seasonal and interannual changes in water storage for continental-scale patterns and for large river basins [Tapley *et al.*, 2004b, Wahr *et al.*, 2004, Andersen and Hinderer, 2005, Andersen *et al.*, 2005, Ramillien *et al.*, 2005, Schmidt *et al.*, 2006].

An alternative method to assess ΔS is to solve the continental water balance equation for this variable. Being the residual value for which errors in the other water balance components accumulate, this approach is constrained to river basins where reliable data of precipitation, runoff, and evapotranspiration are available [e.g., Duan and Schaake, 2003]. The combined atmospheric and terrestrial water balance approach omits the need to explicitly estimate precipitation and evapotranspiration. It resolves for ΔS using atmospheric data on the change of water content and water vapor flux divergence in the atmosphere, and observed river runoff. Recent results of this approach were promising, but the accuracy of the method is limited by errors of the atmospheric data obtained from atmospheric circulation models [Seneviratne *et al.*, 2004; Hirschi *et al.*, 2006].

Still another method to assess water storage change is by using water budget models, which are driven by atmospheric forcing data and simulate hydrological processes and state variables. Such hydrological models for the global scale have been developed for various areas of application, for instance, as soil-vegetation-atmosphere transfer schemes in atmospheric general circulation models (see an overview with regard to soil moisture

simulations in *Robock et al.* [1998]), as soil moisture accounting routines in dynamic global vegetation models (see *Cramer et al.* [2001] for an overview) or for quantification of river discharge and water resources [*Arnell*, 1999; *Vörösmarty et al.*, 1998, 2000; *Döll et al.*, 2003]. The models differ in terms of spatial and temporal resolution, data demand, the detail in process representation, and, consequently, in the way they account for the individual components of the continental water storage. Although the modeling approach is limited by the accuracy of input data and the appropriateness of model formulations and parameterization to represent the actual processes, it allows for spatially distributed results with broad spatial coverage, the differentiation of the various water storage compartments, and for prognostic simulations with changing boundary conditions.

It should be pointed out that only two methods, i.e., the water balance approach and the GRACE mission, which integrate all mass variations that contribute to changes of the gravity field, result in estimates of the total continental water storage change ΔS . All other sources from ground-based measurements, satellite observations and from hydrological models usually deliver data for only one or more selected water storage components. The case study of Illinois [*Rodell and Famiglietti*, 2001] is a rare example where a comprehensive data set of field measurements has been compiled to allow for analyzing the total continental water storage for a large geographic domain. The analysis of global model results in terms of water storage was often restricted to soil moisture, as this was the main storage component of interest for model applications [e.g., *Robock et al.*, 1998; *Dirmeyer et al.*, 1999; *Fan and Van den Dool*, 2004], but also because the modeling domain of many models is limited to the near-surface zone of few meters in depth, omitting deeper groundwater storage. Only recently, in the course of studies related to the hydrological interpretation of GRACE observations (see list of references above), a more comprehensive analysis was performed by adding up simulated storage change of different storage components. In these studies, snow, soil moisture and groundwater storage were added up using the LaD model of *Milly and Shmakin* [2002] and GLDAS of *Rodell et al.* [2004], and, in addition to these three components, surface water storage was taken into account using the WGHM model [*Döll et al.*, 2003].

Both from the data perspective with the limited amount of large-scale observations, and from the modeling perspective where storage change has rarely been analyzed as a model output, there is clearly the need for additional information on continental water storage at the global scale. Also in a geophysical context such as the interpretation of time-variable gravity data, water storage changes are essential for signal separation into oceanic, cryospheric, hydrological and other mass variations. It is desirable to combine and adjust water storage data from the different sources mentioned above in an iterative procedure in order to lead to an improved global picture of water storage, its temporal and spatial variations, and distribution among the various storage components. This study intends to contribute to these aims by reporting on the simulation and analyses of continental water storage with one particular global hydrological model (WGHM). This model stands out relative to most other global models due to representing comprehensively five major components of continental water storage, i.e., water storage on vegetation, storage in surface water bodies, snow, soil water and groundwater storage. Thus, it is conceptually closer than other models to the integral ΔS as derived from GRACE or water balance studies. A short model description and the analyses methods are presented in section 2. Section 3 gives the results for water storage variations at different time scales with global coverage, but also describes the typical storage characteristics of the major global climate zones and large river basins, and the contribution of individual storage components to total storage change.

2. Methods

2.1 Model description

A detailed presentation of the WaterGAP Global Hydrology Model (WGHM), including process formulations, input data, model tuning and validation, is given in *Döll et al.* [2003]. In the following overview, the focus is on the concepts used to represent different continental water storage components in the model. Figure 1 gives an overview on storage compartments and their interactions in WGHM. The model has basically been developed to simulate river discharge within the framework of water availability and water use assessment at the global scale. It simulates the continental water balance on a global grid with $0.5^\circ \times 0.5^\circ$ degree spatial resolution. The model represents the major hydrological processes (snow accumulation and melting, evapotranspiration, runoff generation, lateral transport of water in the river network) by simplifying, conceptual formulations. The modeling time step is one day.

Water storage on the vegetation canopy occurs by interception of precipitation. The capacity of the canopy storage (S_{cmax} , the maximum storage volume that can be accumulated on the canopy) in WGHM is a function of the leaf area index, which varies in space for different land cover types and in time according to the climatic conditions, i.e., the growing seasons. The actual canopy storage S_c is simulated by computing the canopy water balance of total precipitation, throughfall to the soil surface and canopy evaporation E_c . Canopy evaporation is a function of daily potential evapotranspiration E_{pot} (equation 1) [*Deardorff*, 1978], which is computed according to *Priestley and Taylor* [1972].

(1)

$$E_c = E_{pot} \left(\frac{S_c}{S_{cmax}} \right)^{2/3}$$

Snow storage in WGHM is represented by a simple degree-day algorithm. Precipitation is accumulated as snow if the air temperature T is below 0°C . Snow melt M occurs for temperatures above 0°C with daily rates that depend on the land cover type and increase linearly with each degree of exceedance of 0°C (equation 2):

$$M = f_d (T - T_m)$$

(2)

where f_d is the degree-day factor ($2 \text{ mm d}^{-1} \text{ }^\circ\text{C}^{-1}$ in forests and $4 \text{ mm d}^{-1} \text{ }^\circ\text{C}^{-1}$ in other land cover types) and T_m is the threshold temperature for snow melt ($T_m = 0^\circ\text{C}$ is used here). Accumulation of ice and ice mass balances are not accounted for in WGHM, and Antarctica and Greenland are excluded from the simulations.

Water storage in the form of soil moisture in WGHM covers the water content within the effective root zone of the vegetation. Thus, the integration depth for this storage component is spatially variable, depending on the land cover type. Typical values of the effective root depth in WGHM are 1 to 2 m, with a maximum of 4 m for tropical rain forests. The soil water storage capacity S_{smax} is obtained as the product of the root depth and the available water capacity in the uppermost meter of soil [*Batjes*, 1996]. The soil zone is modeled as one layer. Soil moisture storage may change by balancing the input fluxes throughfall precipitation P_{eff} and snowmelt M , on the one hand, with the output fluxes actual evapotranspiration E_a and runoff R_l , on the other hand (Figure 1). Both output fluxes are simulated as a function of the ratio between the actual soil moisture content in the root zone S_s and its storage capacity S_{smax} . In the case of runoff, this non-linear relationship is governed by an exponential

parameter γ (equation 3) which is subject to model tuning against observed river discharge data [Döll *et al.*, 2003].

$$R_l = P_{eff} \left(\frac{S_s}{S_{smax}} \right)^\gamma \quad (3)$$

Groundwater storage in WGHM is represented by a linear storage approach. It is recharged by a fraction of the runoff volume R_l which results as an output flux of the soil water balance described above. Groundwater recharge R_g is variable in space and depends on physiographic characteristics of each model cell, such as topography, soil texture, hydrogeology, and the occurrence of permafrost or glaciers, represented by a recharge factor f_g and the soil texture dependent maximum recharge rate R_{gmax} (equation 4). Groundwater storage is depleted by outflow to river discharge. This groundwater outflow Q_b (mm d⁻¹) is set proportional to the actual volume of groundwater storage S_g (mm) with a globally uniform baseflow coefficient k_b of 0.01 d⁻¹ (equation 5).

$$R_g = \min(R_{gmax}, f_g R_l) \quad (4)$$

$$Q_b = -k_b S_g \quad (5)$$

All groundwater flow in WGHM occurs only within one modeling cell, i.e., there is no transport between the groundwater storages of adjacent cells. Capillary rise or groundwater flow back to the soil zone, as well as evapotranspiration loss from the groundwater storage, are not accounted for.

Water storage in surface water bodies in WGHM comprises surface water in rivers, natural lakes, man-made reservoirs and in wetlands (Figure 1). The global river network is given by the global drainage map of Döll and Lehner [2002], the location of lakes and wetlands within the river network and their spatial extent within each cell are based on the Global Lakes and Wetlands Database (GLWD) of Lehner and Döll [2004]. The storage behavior of the surface water bodies is represented by a cascade of simple linear storage elements. The water balance simulation of each surface water body accounts for inflow from the river network, losses due to evaporation from the water surface, and outflow Q_{out} (m³ d⁻¹) as a function of actual storage volume S_r (m³) with globally uniform storage parameters (outflow coefficient k_r (d⁻¹), maximum active storage depth S_{rmax} (m³)) for each storage type (equation 6). For each surface water body, S_{rmax} is computed as the product of its surface area given in GLWD and the maximum storage depth, set to 5 m for lakes and 2 m for wetlands. In the current WGHM version, reservoir storage dynamics are represented in the same way as for natural lakes.

$$Q_{out} = k_r S_r \left(\frac{S_r}{S_{rmax}} \right)^{1.5} \quad (6)$$

Surface water storage in WGHM is reduced by water withdrawal for consumptive human water use (see Döll *et al.* [2003] for details). The function of rivers is to delay discharge when transported from one modeling cell to another. In the present model version of WGHM, the extent of the lake and wetland water surfaces subject to evaporation does not vary with the actual storage volume due to the lack of adequate global data on surface-volume relationships. Also, the minimum (zero) storage volume in lakes was set to the water level where surface outflow ceases (i.e., where $S_{rmax} = 0$), as no global data on lake volumes were available.

In summary, WGHM accounts for four of the most important continental water storage components: surface water, snow, soil water and groundwater storage. The model does not consider water storage within the biomass which, however, is considerably smaller than any of the other four components. Furthermore, water storage as ice (including permafrost) and in deeper groundwater systems with transport distances beyond the modeling resolution (0.5 degrees) is not accounted for. With regard to storage changes, however, these two components usually have much longer characteristic time scales of variability (decadal and longer) than the other four components. In this paper, with total continental water storage *TWS* we refer to the four major storage components described above.

In this study, the WGHM model is driven with monthly climate variables for 1961-1995 of the Tyndall Centre Climate Research Unit data set CRU TS 2.0 [Mitchell *et al.*, 2004; New *et al.*, 2000], in particular precipitation, wet day frequency, air temperature, and cloudiness. The monthly data are disaggregated within WGHM to daily values. The model was tuned by adjusting the exponent in the soil-moisture accounting routine (equation 3) so that long-term mean annual river discharge matched as closely as possible the observed discharge for 724 large drainage basins worldwide (for details, see Döll *et al.* [2003]). The tuning parameter was regionalized to cells outside of calibration basins using a regression equation relating the parameter to physiographic basin characteristics. For this study, contrary to Döll *et al.* [2003], additional correction factors in river basins where the above tuning did not give satisfactory results of river discharge were not applied in order to maintain closed water balances.

2.2 *Spatial units of analyses*

WGHM model simulations cover the global land area except Antarctica and Greenland. Water storage was analyzed for the major global climate zones according to the Koeppen classification. It uses mean monthly values of air temperature and precipitation, including their seasonality, as classification criteria for climate zones. The Koeppen classification used in this study comprises the five main climate zones and their two or three first-order subtypes, based on the global Koeppen climate map with 0.5 degree resolution by FAO [1997] (Figure 2). Water storage characteristics were also analyzed in this study for the 30 largest river basins worldwide draining into the ocean (size larger than about 700,000 km²), with basin boundaries derived from the global drainage direction map of Döll and Lehner [2002]. In addition, interannual variability of water storage was analyzed at the scale of continents.

2.3 *Statistics of space-time variations of water storage*

Water storage is given in this paper in units of height of an equivalent water column (mm). Total continental water storage *TWS* is computed as the sum of snow, soil moisture, groundwater and surface water storage. Temporal storage variations were analyzed at monthly, seasonal, and interannual time scales for the period 1961-1995. $\Delta TWS_{monthly}$ is the average water storage change between monthly storage values of two subsequent months. $\Delta TWS_{seasonal}$ is the seasonal amplitude of storage change, i.e., the difference between the months with maximum and minimum water storage in a year. The interannual storage change $\Delta TWS_{interann}$ is the water storage change between the same months in subsequent years, averaged for all twelve months of the year.

In addition, an Empirical Orthogonal Functions (EOF) analysis was performed. This multivariate technique is able to identify the dominant simultaneous patterns of space-time variability [Kutzbach, 1967; Preisendorfer, 1988; von Storch and Zwiers, 1999]. To focus the analysis on longer than seasonal variability, long-term monthly means were removed from the

monthly time series of water storage. A spectral analysis of the amplitude (principal component) of the EOFs was carried out to derive the preferred frequencies of storage variations that were described by the EOF patterns. This spectral analysis was performed with a wavelet transformation [Torrence and Compo, 1998], which contrary to the Fourier transformation also conserves the time information. The EOF and spectral analyses were done at the scale of continents.

Additionally, to describe the spatial continuity of water storage patterns, spatial autocorrelograms were determined on a monthly basis. To this end, correlation coefficients as a function of distance between 0.5° grid cells were computed for all pairs of cells grouped into 100 km distance classes. To prevent opposite seasonal signals from merging into single monthly correlograms, the correlograms were calculated separately for each major Koepfen climate zone in the northern and southern hemisphere. Assuming the correlation functions to decay exponentially with distance, the correlation coefficients of each distance group were plotted in a logarithmic scale against distance, and a linear regression line was fitted to them. The negative inverse of the slope of this line is used as an estimator of the scale of spatial dependence in the water storage fields [Entin *et al.*, 2000].

2.4 Sensitivity analysis

A sensitivity analysis of WGHM with regard to uncertainties of model parameters and climate input data was performed. Parameter distributions (uniform, triangular or normal) were defined for each of the 36 model parameters, representing their assumed ranges of uncertainty based on literature data and qualitative reasoning [Kaspar, 2004]. The respective distributions were used globally for each parameter without regional variations of their characteristics. In addition, uncertainty ranges for the WGHM climate input data were defined. For monthly precipitation, the lower bound of the uncertainty range was set to the value given in the CRU data set, the upper bound was set to this value multiplied by the correction factor for systematic precipitation measurement errors defined by Legates and Willmott [1990]. For the number of rain days per month, an uncertainty range of ± 2 days was assumed. To monthly mean temperature, a normal distribution with $2\sigma = 2^\circ\text{C}$ and to sunshine duration a normal distribution with $2\sigma = 25\%$ were assigned. 2000 Monte-Carlo runs were done with the WGHM model for 22 of the largest river basins, with the parameter sets defined from the above distributions by Latin-Hypercube-Sampling. As a measure of model sensitivity, the rank correlation coefficient after Spearman (r_{spear}) between parameter values and seasonal total water storage change ($\Delta TWS_{seasonal}$) was used. To facilitate the interpretation of the results, the 36 model parameters were assigned to different process categories, depending on the equations in which they are implemented in the model: radiation and evaporative demand of the atmosphere (7 parameters), interception storage (6 parameters), snow accumulation and melt (5 parameters), soil water storage (2 parameters and the tuning parameter γ), groundwater recharge and storage (6 parameters), surface water dynamics in rivers, lakes and wetlands (9 parameters).

3. Results and Discussion

3.1 Total storage volumes

Total continental water storage *TWS* is illustrated in its global distribution for the period 1961-95 in Figure 3. It should be noted that total water storage here refers to the storage of precipitation water fallen after 1960 and does not account for older waters in deep groundwater and lakes. *TWS* varies markedly among the major global climate zones (Table 1). In general, mean annual *TWS* tends to be larger in areas with a more positive climatic water balance (precipitation minus evapotranspiration) which provides larger volumes of water for temporary storage in subsurface and surface water bodies. This applies in particular for humid tropical zones with high rainfall (e.g., climate Af) and for cold, humid climates with low evaporation (e.g, climate D). Within the climate zone, areas of climate sub-types with distinct dry periods have below-average storage volumes (in particular climates Aw, Cs, Dw). *TWS* is lowest in dry climates where the comparatively low precipitation volumes are to a large part quickly returned to the atmosphere by evapotranspiration.

Storage in surface waters (wetlands, reservoirs, lakes and rivers) contributes a large proportion of about 35-60% to *TWS* in all climates, with more than 50% globally (Table 1). In particular, extensive wetland and lake areas in high northern latitudes which attain nearly 20% of the total land area (climate Df, Table 1) play an important role for the comparatively large mean annual *TWS* of that region. In the tropical, dry and temperate climate zone, surface water storage in wetlands exceeds mean annual storage volumes in lakes and reservoirs. Surface water storage in rivers generally is of minor importance when averaged for large areas. Locally, however, it can represent an important storage component as is illustrated by the linear features along major rivers with high discharge volumes (Figure 3).

The contribution of soil moisture and groundwater storage to *TWS* is largest in the comparatively wet tropical and temperate climate. Within each climate, the contribution of soil moisture is larger relative to groundwater for the areas with wetter climate sub-types (such as Af and Cf). High precipitation during the season with high evaporation rates (in summer for climate Cw), in contrary, reduces the contribution of soil moisture to *TWS* when compared with a climate where major precipitation coincides with low evaporation and, thus, allows for the replenishment of soil moisture storage (climate Cs). In the cold and polar climate, soil moisture storage is more important than groundwater storage which may be related to the assumption of no groundwater recharge in permafrost areas in WGHM. In these two climate zones, snow storage is a major contribution to *TWS*. A minor snow contribution to *TWS* occurs also in the dry climate zone B, resulting from snowfall in cool mid-latitude steppes and deserts. Interception storage on plant surfaces was found to be negligible in all climate zones (not shown).

For comparison, also the basin-average mean annual *TWS* of the selected large river basins are shown in Table 2. These *TWS* values often aggregate storage characteristics of several climate zones due to the large spatial extent of the basins. Among the basins that stick out with very high *TWS* values are those with large surface water storage capacity such as the Saint-Lawrence basin that includes the North-American Great Lakes area or the Canadian Nelson basin, but also many tropical basins with extended wetland zones, such as the Amazon, Orinoco and Tocantins basin.

It should be noted that absolute storage volumes as given here are model-specific and depend, beside of the representation of process dynamics, on the definition of the water storage capacity for a certain storage component. Differences among models will occur particularly

for soil moisture storage, as the depth of the soil zone may vary considerably between models (see, e.g., the ranges for large river basins given in Rodell & Famiglietti [1999]). Differences in the depth of the lower soil boundary will in particular alter the partitioning between soil moisture and groundwater storage. In addition, the definition of surface water storage capacity can be expected to have a strong impact on absolute water storage estimates, although to the authors' knowledge there exists no other large scale assessment for this storage component so far. Nevertheless, storage capacities are given in Table 1 for the soil zone (S_{smax}) and for surface water bodies (lakes and wetlands, S_{rmax}) to serve as a basis for comparisons with other models or data sets, and for the analysis of storage variations for which the assumed storage capacity sets an upper boundary (see section 2.1 for the definition of S_{smax} and S_{rmax} for the WGHM model).

3.2 *Monthly and seasonal variations of water storage*

Seasonal variations of water storage $\Delta TWS_{seasonal}$ are largest for the tropical climate zone according to the simulation results (Table 3, Figure 4). The main reason are the monsoon-type rainfall characteristics of many tropical environments with overall high mean annual precipitation but large differences in rainfall volumes between dry and wet seasons (Table 3). Among those, the lowlands of the southern Amazon and the lower Tocantins basins, and widespread areas in South-East Asia exhibit some of the largest seasonal storage amplitudes worldwide, with storage difference between the wettest and driest month exceeding 250 mm, in areas with high accumulation of surface water in the wet season exceeding 400 mm (Figure 4). Central tropical areas close to the equator such as in the central Amazon and Congo basins, characterized by a more uniform distribution of precipitation throughout the year (climate Af), often have smaller storage amplitudes than the adjacent areas in the marginal tropics. In spite of a strong seasonality of precipitation, tropical areas with a long dry season (climate Aw) have comparatively lower seasonal $\Delta TWS_{seasonal}$ due to overall lower rainfall volumes also in the wet season.

TWS variations for the temperate, cold, and polar climate zones are in the same order of magnitude both for the monthly and seasonal time scale. Within the temperate zone, the Mediterranean climate sub-type (climate Cs) shows the lowest storage variations. In contrast to the temperate zone, changes in snow storage make up a large part of TWS variations in the cold and polar (D and E) climate. A high spatial variability in TWS changes occurs within these snow-dominated climate zones. In particular, cold maritime zones with high precipitation volumes in winter and thus a considerable accumulation of water storage in the form of snow until the snowmelt in summer exhibit very high seasonal storage amplitudes. The coastal mountain range of western Canada and Alaska, parts of eastern North America, and the west coast of Scandinavia are among the areas with the largest storage amplitudes worldwide, exceeding 400 mm. Roughly in line with a decreasing gradient of snow precipitation in winter from the west (climate Df) to the east (climate Dw) in Northern Asia, the temporal storage variations also tend to decrease from west to east in that area. At the global scale, storage variations are by far the smallest in the dry climate zone B due to the overall small water availability.

The contributions of individual storage components to seasonal TWS variations differ considerably among the different climate zones (Table 3). Change in snow storage between the winter and the summer season is the dominant process to explain seasonal storage variations in the cold and polar climate zone D and E. Both the temperate and the tropical climate zone are dominated by variations in the soil and groundwater storage. In the dry

climate, variation of surface water storage is the most important contribution to seasonal *TWS* change, similar to the large fraction of this storage component on mean *TWS* (compare Table 1). In the other global climate zones, in contrast, in spite of a large contribution of surface water to *TWS* (more than 40%), its contribution to seasonal *TWS* variations is comparatively smaller. For all climate zones, the contribution of groundwater storage variations to *TWS* variations and the temporal groundwater variations in absolute values (Table 4) are smaller than those of soil water storage, although soil water and groundwater build a similar fraction on mean absolute storage volume (Table 1). This is in line with a usually more dynamic behavior of hydrological processes close to the land surface, where the soil water storage is more directly exposed to climatic forcing by precipitation and evaporation, to water extraction by vegetation, and where water movement often is faster due to higher hydraulic conductivities.

Another reason for a small contribution of a certain water storage component to seasonal *TWS* variations as given in Table 3 is that the seasonal water storage cycle of the individual storage component can be shifted in time relative to the *TWS* seasonal cycle. Thus, the full seasonal storage amplitude of an individual component ($\Delta S1$ in Table 4) often is larger than when taken for the months of the *TWS* maximum and minimum ($\Delta S2$). The maximum of groundwater storage, for instance, often is delayed relative to the maximum of soil water storage due to the later arrival of infiltrating water in the groundwater and due to longer residence times of water in the groundwater zone. This behavior is illustrated for most large river basins as shown in Figure 5. The maximum of soil water storage and surface water storage in turn is delayed relative to the maximum of snow storage, as the soil is primarily wetted up and surface water bodies are filled up during extensive snowmelt, i.e., decrease in snow storage, in spring (see, for instance, the linear patterns in Figure 6 along major rivers in Northern Asia with maximum storage volumes that are delayed relative to the surrounding land areas). In snow-dominated river areas and in the cold climate region in general, the seasonal cycle of groundwater storage is opposite to the *TWS* cycle which is dominated by the cycle of snow storage. As an example of a large river basin, these different dynamics of storage components are shown in Figure 5b for the Yenissei basin. Overall, differing seasonal cycles of individual storage components lead to a dampening of the seasonal *TWS* amplitude, expressed in negative values for their contribution to seasonal ΔTWS in Tables 2 and 3.

For the largest river basins worldwide, the tropical streams of South American (Amazon, Orinoco, Tocantins) are among those with the largest seasonal water storage change worldwide in the order of 200-300 mm (Table 2). While their mean annual *TWS* is very similar to each other, the Tocantins and Orinoco basins have even larger seasonal storage amplitudes compared to the Amazon. The reason is that the Amazon basin extends over both hemispheres with the rainy season and related water storage maxima occurring during different periods of the year (Figure 6). When averaging for the entire basins, storage changes of opposite direction level out to some extent. In contrary, the Tocantins and Orinoco basins are completely located on the Southern and Northern Hemisphere, respectively, with a more homogeneous seasonal cycle throughout the basin. The comparatively small seasonal ΔTWS in the equatorial Congo basin is partly due to a similar compensation effect as for the Amazon. Another at least partly tropical basin with very high seasonal ΔTWS is the Ganges/Brahmaputra basin of which the dynamics are driven by the strong rainfall seasonality of the Indian monsoon. Several higher latitude basins, in particular Ob, Mackenzie, Volga, Nelson, Saint-Lawrence and Columbia, show high seasonal ΔTWS above 100mm, dominated

by the seasonal dynamics of snow storage. Many river basins in the temperate climate, and in particular those pertaining to dryland areas, have a low seasonal ΔTWS below 100mm.

It should be noted that many large river basins span several climate zones (Figure 2) with different seasonal dynamics of their water storage so that storage changes in one zone may be compensated by opposite changes in another zone. In addition, as explained above, the seasonal cycles of individual storage components may be out of phase relative to each other so that the seasonal amplitude of total water storage is attenuated. In many river basins, this is the case for groundwater storage, but partly also for surface water storage when shifted in time relative to snow storage (negative values in Table 2).

3.3 *Interannual variations of water storage*

Interannual storage variations ($\Delta TWS_{interann}$) are small compared to the seasonal variations for all climates according to the WGHM results (Table 3). In absolute values, $\Delta TWS_{interann}$ is largest for the tropical climate and lowest for the dry climate zone. Relative to total storage volume TWS , however, the interannual variability is most pronounced in the dry climate zone, reflecting the comparatively high irregularity of rainfall in those areas.

The major difference in the contribution of the individual storage components to interannual storage change (Table 5) as compared to their contributions to the seasonal storage change (compare Table 3) is the markedly less important contribution of snow storage to the interannual signal. Instead, groundwater storage and partly also surface water storage in lakes and wetlands (but not in rivers) contribute a larger fraction to interannual storage change. This illustrates the shift from storage components with short water residence times (such as snow and river storage with typically seasonal dynamics) to those with longer residence times (especially groundwater) when long-term water storage variations are of concern.

Figure 7 shows the results of the continental-scale EOF analysis of storage variations for the example of South-America. The first EOF explains 24.3% of the total space-time variability of water storage in South-America at longer than seasonal time scales (the seasonal variability has been removed from this analysis, see section 2.3). The pattern of variability (Figure 7a) shows negative anomalies in the southern parts of the continent, particularly along the Paraná River and its inundation areas. In contrast, in the northern parts of South-America positive anomalies prevail, corresponding to an increase in water storage. The entire Amazon basin and the main stretches of the Amazon river and its tributaries stick out with particularly strong positive anomalies. The wavelet spectrum of the corresponding EOF amplitude (Figure 7b) indicates that these space-time variations can be attributed to the El Niño Southern Oscillation (ENSO) as confirmed by various publications [e.g., *Ropelewski and Halpert, 1987, Aceituno, 1988, Vuille, 1999, Waylen and Poveda, 2002*]. The strongest variation of the 1.EOF amplitude occurs between 1983 and 1986, coherent with the strongest El Niño event in the analyzed time period in 1983. With 24-30 months, the frequency of this significant signal is somewhat higher than the typical ENSO frequency (30-60 months), and the comparison of the amplitude of the 1.EOF with a typical ENSO index, the NINO3 timeseries (Fig. 7b) shows some discrepancies, but the time-coherency is obvious. Furthermore, some parts of the South American hydro-climatology, in particular the Pacific coastal areas, are strongly affected by sea surface temperature (SST) anomalies off the coast of Ecuador and Peru (NINO1+2 index area) [*Stuck et al., 2006*], while the typical ENSO indices are based on central Pacific SST anomalies (NINO3 & NINO3.4). Those off-coastal SST (NINO1+2) underlie an additional more frequent variation with a period of nearly two years. Thus, the pattern of the 1.EOF can

be considered as a possible reaction of continental water storage to El Niño events, like the 1983 one and its biennial regional modulation.

An even more clear dependency on ENSO was obtained for the Australian continent, including New Zealand and the Indonesian islands (Figure 8). The strongest El Niño events of 1983, 1973 and 1965/66 are well pronounced in the corresponding amplitude of the 1.EOF (Figure 8b), which is highly correlated with the typical indices of ENSO (e.g., NINO3). Over the Australian continent, only weak variations of water storage were derived except for negative anomalies at the eastern and the northern coastal zone (Figure 8a). The anomalies for Indonesia and New Zealand are much stronger with negative values in the equatorial regions and positive values over the southern island of New Zealand. These results are in good agreement with the well-known droughts in the Indonesian and North-Australian region during El Niño events [e.g. *Ropelewski and Halpert, 1987, Chiew et al., 1998*].

For Europe, the 1.EOF variability explains nearly one third of the total variability and shows generally positive anomalies in central and north-eastern Europe and negative anomalies in the Mediterranean and Balkans region, and in Norway (Figure 9). This European pattern and its corresponding spectral behavior may indicate that this 1.EOF of water storage corresponds to precipitation anomalies due to the North Atlantic Oscillation (NAO). The positive phase of the NAO leads to an intensification of the west wind drift due to a reinforcement of the Iceland low and the Azores high pressure systems, in particular in the boreal winter months [*Wallace and Gutzler, 1981; Barnston and Livezey, 1987*]. This in turn causes positive precipitation anomalies in central Europe and negative anomalies in southern Europe and at the Norwegian coast, reflected in the water storage variations. The mean winter (JFM) timeseries of the NAO index (Fig. 9b) give an indication for this linkage. The NAO typically occurs on time scales ranging from interannual to decadal [e.g., *Hurrell et al., 2003*], which is in accordance with the spectral behavior of the EOF amplitude shown by the wavelet spectrum (Figure 9b).

For the other continents, the interannual water storage variability is superposed by long-term trends. For instance, a decreasing trend in the Sahel zone of Africa is seen, which is conform to the observed trend in precipitation. A decreasing (increasing) water storage trend was found in northern Asia (northern America), corresponding to trends in the CRU precipitation data used as model input (not shown).

At the global scale, total continental water storage simulated by WGHM shows a maximum in the mid-1970s and a decreasing trend until the end of the study period in 1995 (Figure 10b). This tendency is related to the precipitation volumes on the continents used as model input (Figure 10a). A similar behaviour is found for land water storage and soil moisture simulated with other global models by *Ngo-Duc et al. [2005]* and *Fan and van den Dool [2004]*. However, the ORCHIDEE model used in *Ngo-Duc et al. [2005]* shows larger storage amplitudes at the interannual scale than WGHM (Figure 10c). The LaD model of *Milly and Shmakin [2002]* for 1980-1995 is of intermediate interannual variability. While it shows some similarity in the overall anomaly pattern, several years differ from the WGHM and ORCHIDEE behavior. The closer correspondence in the interannual sequence between WGHM and ORCHIDEE is presumably due to the same precipitation forcing data (CRU) used by both models. Differences between models in terms of the magnitude of interannual variability can be due to different water storage compartments represented in the models, different definitions for them (i.e., depth of the soil water zone), and different modeling concepts. According to WGHM results, water storage in surface water bodies has the most important contribution to the interannual/decadal variations, followed by groundwater and

soil moisture. Snow storage, in contrary, does not explain a significant part of total continental storage variations. This ranking among the storage components is also similar to the results of *Ngo-Duc et al.* [2005], although they aggregated groundwater and surface water into one storage component.

3.4 Spatial continuity of water storage

Spatial autocorrelograms of water storage were computed for each major Koeppen climate zone. When considering the sum of snow, soil moisture and groundwater storage, an approximately exponential decay of the correlation with distance was found for all climate zones (Figure 11a). The mean correlation length for monthly fields was in the range of 400 – 900 km, with a tendency of shorter correlation lengths in colder climates (Table 6). These correlation lengths compare well with scales of about 500 km given for soil moisture in extratropical areas by *Entin et al.* [2000]. Slightly larger scales derived here based on WGHM may be caused by including groundwater storage which is usually less variable in space as compared to soil water.

If surface water is added to snow, soil moisture and groundwater storage, the spatial continuity of the fields is considerably lower (Figure 11b). The autocorrelation functions show small values already for the first distance class, indicating that total water storage in two adjacent 0.5° degree cells often is dissimilar. One reason is that huge volumes of water are stored within a small domain due to the comparatively narrow shape of surface water bodies, such as rivers or floodplains. Another reason is that the storage dynamics of surface water bodies in large river basins can be uncorrelated to the dynamics of surrounding land areas because they are dominated by inflow from upstream basin areas with a different hydrological regime. The spatial correlation function of total water storage including surface water cannot be described by an exponential autocorrelation model over its full range due to its sharp decay at short distances. When only including the correlation values of the first three distance groups for the linear regression of logarithmic values, correlation lengths were lower than 200 km (Table 6).

The spatial correlation characteristics of monthly storage change were in general similar to those of absolute monthly water storage (Table 6). In particular, spatial continuity decreased considerably if surface water storage change was included in addition to ground, soil and surface water. Slightly higher correlation lengths for ΔTWS as compared to TWS indicate that the spatial anomalies caused by surface water bodies are reduced, although still prominent, if relative instead of absolute storage values are considered.

In addition, correlation lengths of water storage vary seasonally (Table 6, Figure 12). For the example of water storage in the temperate climate zone of the northern hemisphere, maximum spatial continuity occurs in winter (when the actual water storage is at its maximum), minimum correlation exists in spring and autumn with the transition from wet to dry stages, and a secondary maximum of correlation lengths in summer with comparatively dry conditions over larger areas.

3.5 Reliability of results

Simulation results of continental water storage with WGHM, similar to the results of other models, are subject to a wide range of uncertainties. Among those are uncertainties of model structure and process formulations, model parameters, and input data. Particularly with regard to the output variable water storage, a rigorous model validation is hardly feasible at large scales due to the lack of independent data / observations. Nevertheless, a tentative evaluation

of model results may comprise (1) a model-alone sensitivity analysis for uncertainties of parameters, input data, and model structure, (2) the model validation with respect to other water balance variables, in particular river discharge, (3) a comparison to water storage results of other global models, (4) a comparison with water storage change estimates from water balance studies, (5) a comparison with observational data, in particular mass variations derived from the GRACE satellite mission.

(1) For 22 large river basins, the sensitivity of WGHM simulation results in terms of seasonal water storage change $\Delta TWS_{seasonal}$ for parameter and climate input uncertainty was analyzed (see section 2.4). For each basin, the most sensitive parameters were identified according to the criterion $|r_{spear}| > 0.2$. From this, a subset of 2 to 7 parameters resulted in each basin. The results show considerable regional differences of parameter sensitivities (Table 7). The most sensitive parameters in a specific river basin are mainly those that govern the dynamics of the most important water storage compartments in the selected basin (compare Table 2). For instance, in many high- and mid-latitude basins where snow storage variations account for an important part of $\Delta TWS_{seasonal}$, uncertainties of parameters of the snow-melt routine are highly sensitive on model results.

In river basins with high discharge volumes (e.g., Amazon, Congo, Yangtze), parameters describing the dynamics of surface water bodies, in particular river flow velocity, and parameters describing lake dynamics in basins that are characterized by numerous lakes and wetlands (e.g. Saint-Lawrence, Paraná), are the most sensitive. Uncertainty of soil water parameters (soil storage capacity, root depth) is relevant in particular in river basins in the temperate zone (e.g., Mississippi, Danube) and in dryland areas (e.g., Nile, Niger, Oranje) where water storage processes in the soil prevail. The runoff tuning parameter γ shows a significant effect on water storage changes for several river basins, illustrating its crucial role in relating runoff generation to soil moisture dynamics. Uncertainty of radiation and evaporation parameters is of widespread relevance for model results, with emphasis on tropical river basins where the atmospheric evaporative demand is high with an important impact on the water balance and storage changes. In contrast, parameter uncertainty with regard to interception and groundwater processes has a comparatively small effect on simulated $\Delta TWS_{seasonal}$ for the given WGHM model structure.

Among uncertainties of climate input data, the effect of precipitation uncertainty clearly is the most prominent one. While it is comparatively less important for the tropical basins, it has a very strong effect in snow-dominated basins (Table 7), where precipitation measurement errors are particularly high due to a large fraction of snow precipitation and the systematic undercatch of solid precipitation by turbulence effects at ground stations. Compensating this effect by precipitation correction factors, changes in the precipitation input in the winter season cause marked changes in snow accumulation and markedly affect the seasonality of TWS . Model sensitivity for $\Delta TWS_{seasonal}$ to uncertainty of other climate data is considerably lower, with some effects of uncertain air temperature on melt processes in snow-influenced basins (Danube, Yukon).

The sensitivity of WGHM simulation results in terms of $\Delta TWS_{seasonal}$ for uncertainty of model parameters and climate input data is summarized in Table 7 (last column). The standard deviation of $\Delta TWS_{seasonal}$ for the 2000 Monte-Carlo runs is in the range of 6 to 30 % of mean $\Delta TWS_{seasonal}$ for the selected large river basins. It has to be emphasized that complete model uncertainties may be higher due to errors of model structure. A full sensitivity analysis, however, is beyond the scope of this study.

(2) Validation of WGHM against observed river discharge for more than 700 stations worldwide demonstrated that generally reliable results were obtained for large river basins [Döll *et al.*, 2003]. For many areas, reasonable runoff simulations may be an indicator that also storage change is reasonably represented in the model since both variables are directly linked via the water balance equation. Nevertheless, care should be taken when generalizing this assumption because the other variables in the water balance equation (precipitation and evapotranspiration) are subject to large errors, and because hydrological models may in some cases result in correct runoff simulations for the wrong reason, incorrectly representing internal river basin states such as soil moisture, for instance. In addition, Döll *et al.* [2003] pointed out specific basin types where WGHM tended to give worse results in terms of river discharge. This can be an indication that also water storage simulations are less reliable in these regions. In particular, these are semi-arid and arid basins where some typical evaporation processes (such as transmission losses from river channels) are not represented by the model, which could finally lead to an overestimation of simulated water storage. Surface water storage simulations with WGHM are generally highly uncertain, mainly because there is not enough information available to describe satisfactorily the dynamics of wetlands and inundation areas along major rivers, and because the management behavior of man-made reservoirs, water basin transfers or irrigation schemes are not sufficiently known to accurately represent surface water dynamics in highly developed river basins. Furthermore, the accuracy of water storage simulations generally is limited by the accuracy of the climatic forcing data of the model, of which precipitation is the most critical variable. For example, in data sets based on ground measurements such as the CRU data used here, there is a systematic underestimation of precipitation in regions with a large contribution of snow (see above). In these snow-dominated basins such as in Siberia and North America, the seasonal storage change simulated by WGHM will probably be underestimated due to the underestimated snow accumulation during the winter season.

(3) As most other global models do not calculate water storage in the comprehensive sense of WGHM (including surface water storage, for instance), their results are not directly comparable to WGHM for purposes of model evaluation. To our knowledge, the only example of analogous water storage data has been given for the ORCHIDEE land surface model in Ngo-Duc *et al.* [2005], to which WGHM shows good correspondence in terms of the interannual storage dynamics (see above).

(4) Seasonal water storage change of WGHM for the largest river basins was compared to storage change from combined atmospheric-terrestrial water balance studies as a further way of model evaluation (Table 8). In this approach, total water storage change is derived by balancing atmospheric water vapor flux convergence and atmospheric water content based on forecast or re-analysis data of atmospheric circulation models with observed river discharge for large river basins. Studies used here covering several large river basins worldwide are those of Oki *et al.* [1995] (OK) (cited in Rodell and Famiglietti [1999], Table 4), Masuda *et al.* [2001] (MA) using NCEP/NCAR reanalysis data, and Hirschi *et al.* [2006] (HI) using the ECMWF ERA-40 reanalysis product. While the data of Oki *et al.* [1995] cover the period 1989-92 only, the overall time span of the analyses of Masuda *et al.* [2001] and Hirschi *et al.* [2006] was from 1973-1995 and 1958-2000, respectively, although for several river basins the effective period was shorter due to limited availability of runoff data (see their papers for details). The values in Table 8 represent the seasonal storage change as the difference between the maximum and the minimum of the climatologic mean monthly water storage. Therefore, the values for WGHM are slightly lower than $\Delta TWS_{seasonal}$ given in Table 2.

For most river basins, WGHM has considerably lower values than the *OK* results. However, as *OK* storage change is also markedly larger than both *MA* and *HI* for many basins, it may represent overestimated values for certain reasons. WGHM results are much closer to *HI* and *MA* results, which in turn are very similar to each other for nearly all basins, except for the Murray-Darling and Amudarya/Syrdarya where *HI* gives much higher values. In an overview for all basins worldwide, there is no clear tendency of an over- or underestimation by WGHM compared to *HI* and *MA* and an overall reasonable correspondence. Nevertheless, there is a large scatter between the data sets with some typical patterns of large deviations: WGHM storage change is often considerably smaller than *HI* and *MA* for river basins in northern latitudes such as Yensissei, Ob, Lena, Yukon and Columbia River. The reason presumably is the underestimation of snow precipitation in WGHM as mentioned in the previous paragraph. There is also a marked underestimation of seasonal storage change by WGHM in some river basins comprising arid areas, such as Amudarya/Syrdarya, Euphrates and Indus, which could be due to badly represented dryland hydrological processes or to strong water use impacts. Clearly higher values of WGHM in comparison to *HI* and *MA* appear for some river basins that are strongly influenced by large natural and/or man-made lakes (Volga, Nelson, Saint-Lawrence River) which might be an indication of deficiencies of WGHM to represent this surface water storage component. On the other hand, also storage change results of the water balance studies are subject to errors by limitations of the atmospheric data such as underestimations of moisture convergence [Hirschi et al., 2006] or difficulties to represent mountainous areas. Additionally, both different analysis time periods and non-identical basin areas may partly explain deviations between WGHM and the water balance data.

(5) The comparison of WGHM monthly to seasonal storage change to first results of the GRACE satellite mission (launched in 2002) at the global scale by *Schmidt et al.* [2006] showed overall similar spatial patterns but less temporal storage variations for WGHM than for the mass variations by GRACE that were previously reduced to the hydrological signal component. Also *Ramillien et al.* [2005] found for their GRACE solutions a good agreement to WGHM in terms of the geographical location of seasonal storage anomalies, but significant differences in the amplitudes of storage change. These differences, however, did not show a systematic underestimation by WGHM but the sign depended on the region. The comparison to GRACE results gave first ideas on WGHM limitations similar to those obtained for the other evaluation approaches above. Hydrological signals from GRACE, in turn, are subject to instrument and solution errors, residual signals and aliasing effects of other than hydrological mass variations, and they suffer signal leakage from surrounding areas when analyzed for specific regions such as river basins (see, e.g., Seo and Wilson [2005] for an overview on error sources when resolving GRACE fields for hydrological signals). These features still limit the value of GRACE data for a rigorous validation of hydrological models at the moment.

4 Conclusions

While the simulated fields of continental water storage in this study based on WGHM do not comprise the contributions of ice and deep groundwater, they nonetheless represent a comprehensive summation of the most important storage compartments by including snow, soil moisture, groundwater and surface water in rivers, lakes, reservoirs and wetlands. In this respect, the WGHM water storage data go beyond those of most other global land surface models, and they are comparable to what is obtained in terms of total water storage change from water balance studies or from time-variable gravity data of the GRACE satellite mission. Seasonal variations represent the dominant time-variable signal of water storage change. At the interannual scale, a considerable part of the variations can be associated with large-scale oscillations such as ENSO or NAO. In general, tropical and high-latitude regions exhibit the strongest storage variations. The contribution of individual storage compartments to total storage change varies considerably among the climate zones, with snow storage dominating the signal in cold and polar regions, and soil water in the temperate and tropical zone. Groundwater storage change tends to have a larger contribution to total storage change for interannual than for seasonal storage dynamics due to longer water residence times.

Besides, surface water makes a considerable contribution to total storage change according to the WGHM results in nearly all regions. This expands earlier results such as by *Matsuyama and Masuda* [1997] showing a predominance of surface storage change on the seasonal signal in the Amazon basin, or by *Alsdorf et al.* [2003] arguing for the large seasonal variability of surface water storage when compared to soil moisture on the African continent. Thus, for a valid comparison of total continental water storage change such as from GRACE with simulation results of land surface models, the surface water compartment has to be included in the model estimates. The consideration of additional water storage compartments, however, does not necessarily result in larger amplitudes of storage variations. As shown here, a seasonally shifted phase of groundwater dynamics relative to soil moisture and surface water, for instance, may have a dampening effect on total storage amplitudes.

Surface water storage in rivers, wetlands and lakes is characterized by a high spatial variability compared to other storage compartments. This has a considerable impact on the degree of spatial continuity of large-scale water storage fields. While for the sum of snow, soil moisture and groundwater storage spatial correlation lengths of 400 – 900 km were found, the correlation length dropped to values below 200 km if surface water storage was added to the fields. These short correlation lengths should be considered for extracting regional water storage variations from GRACE gravity data with filtering methods that need an a priori estimate of the spatial correlation function of the expected storage signal [*Swenson and Wahr*, 2002]. Also, the inappropriateness of an exponential function due to the observed sharp decay at short distances should be examined in this context. In practical terms, the short correlation lengths tend to increase the contribution of satellite measurement errors and to decrease the contribution of leakage errors to the total error budget of regional solutions. In total, however, this may enhance or reduce the final accuracy of storage estimates from GRACE, depending on the location and size of the area under consideration [*Swenson et al.*, 2003].

In general, while storage change results from WGHM globally agree well with data from other sources, there remain numerous uncertainties and limitations in large-scale modeling of continental water storage. Model sensitivity to uncertainties of individual parameters and input data varies regionally with the relevance of specific storage compartments on water

storage variations. To advance, inter-comparisons with other global models that preferably encompass a similarly large range of water storage compartments should be undertaken. In particular, a more rigorous model validation against observational or combined observation-model-based data is required, including the combined water balance approach and time-variable gravity data such as from GRACE, but also calling for other large-scale water storage observations such as by satellite missions dedicated to surface water bodies [Alsdorf *et al.*, 2003].

References

- Alsdorf, D., D.P. Lettenmeier, and C. Vörösmarty (2003), The need for global, satellite-based observations of terrestrial surface waters, *Eos Trans. AGU*, 84(29), 269-276.
- Alsdorf, D.E., J.M. Melack, T. Dunne, L.A.K. Mertes, L.L. Hess, and L.C. Smith (2000), Interferometric radar measurements of water level changes on the Amazon flood plain, *Nature*, 404, 174-177.
- Andersen, O. B., and J. Hinderer (2005), Global interannual gravity changes from GRACE: Early results, *Geophysical Research Letters*, 32, L01402, doi:01410.01029/02004GL020948.
- Andersen, O. B., S. I. Seneviratne, J. Hinderer, and P. Viterbo, GRACE-derived terrestrial water storage depletion associated with the 2003 European heat wave (2005), *Geophysical Research Letters*, 32, L18405, doi:18410.11029/12005GL023574.
- Arnell, N.W. (1999), A simple water balance model for the simulation of streamflow over a large geographic domain, *Journal of Hydrology*, 217, 314-335.
- Batjes, N.H. (1996), Development of a world data set of soil water retention properties using pedotransfer rules, *Geoderma*, 71 (1-2), 31-52.
- Bevis, M., D. Alsdorf, E. Kendrick, L. P. Fortes, B. Forsberg, R. Smalley Jr., and J. Becker (2005), Seasonal fluctuations in the mass of the Amazon river system and Earth's elastic response, *Geophysical Research Letters*, 32, L16308, doi:16310.11029/12005GL023491.
- Birkett, C.M. (1998), Contribution of TOPEX NASA radar altimeter to the global monitoring of large rivers and wetlands, *Water Resources Research*, 34 (5), 1223-1239.
- Birkett, C.M., L.A.K. Mertes, T. Dunne, M. Costa, and J. Jasinski (2002), Altimetric remote sensing of the Amazon: Application of satellite radar altimetry, *Journal of Geophysical Research*, 107 (D20), 8059, 10.1029/2001JD000609.
- Cazenave, A., F. Mercier, F. Bouille, and J.M. Lemoine (1999), Global-scale interactions between the solid Earth and its fluid envelopes at the seasonal time scale, *Earth and Planetary Science Letters*, 171 (4), 549-559.
- Chiew, F.H.S., T.C. Piechota, J.A. Dracup, and T.A. McMahon (1998), El Niño/Southern Oscillation and Australian rainfall, streamflow and drought: links and potential for forecasting, *J. Hydrol.*, 204, 138-149.
- Cramer, W., A. Bondeau, F.I. Woodward, I.C. Prentice, R.A. Betts, V. Brovkin, P.M. Cox, V. Fisher, J. Foley, A.D. Friend, C. Kucharik, M.R. Lomas, N. Ramankutty, S. Sitch, B. Smith, A. White, and C. Young-Molling (2001), Global response of terrestrial ecosystem structure and function to CO₂ and climate change: results from six dynamic global vegetation models, *Global Change Biology*, 7, 357-373.
- Deardorff, J. W. (1978), Efficient prediction of ground surface temperature and moisture, with inclusion of a layer of vegetation, *Journal of Geophysical Research*, C86, 1889-1903.
- Dickey, J.O., C.R. Bentley, R. Bilham, J.A. Carton, R.J. Eanes, T.A. Herring, W.M. Kaula, G.S.E. Lagerloef, S. Rojstaczer, W.H.F. Smith, H.M. Van den Dool, J. Wahr, and M.T. Zuber (1999), Gravity and the hydrosphere: new frontier, *Hydrological Sciences Journal*, 44 (3), 407-416.
- Dirmeyer, P., A.J. Dolman, and N. Sato (1999), The Global Soil Wetness Project: A pilot project for global land surface modeling and validation, *Bull. Am. Meteorol. Soc.*, 80, 851-878.
- Döll, P., and B. Lehner (2002), Validation of a new global 30-min drainage direction map, *Journal of Hydrology*, 258 (1-4), 214-231.
- Döll, P., F. Kaspar, and B. Lehner (2003), A global hydrological model for deriving water availability indicators: model tuning and validation, *Journal of Hydrology*, 270, 105-134.
- Duan, Q., and J.C. Schaake (2003), Total water storage in the Arkansas-Red River basin, *Journal of Geophysical Research*, 108 (D22), 8853, doi: 10.1029/2002JD003152.

- Entin, J. K., A. Robock, K. Y. Vinnikov, S. E. Hollinger, S. Liu, and A. Namkhai (2000), Temporal and spatial scales of observed soil moisture variations in the extratropics, *Journal of Geophysical Research*, *105*, 11865-11877.
- Fan, Y., and H. van den Dool (2004), Climate Prediction Center global monthly soil moisture data set at 0.5° resolution for 1948 to present, *Journal of Geophysical Research*, *109*, D10102, doi:10.1029/2003JD004345.
- FAO (1997), *Koepfen's Climate Classification Map*, Food and Agriculture Organization of the United Nations (FAO), Sustainable Development Department, Agrometeorology Group, <http://www.fao.org/WAICENT/FAOINFO/SUSTDEV/EIdirect/CLIMATE/EIsp0002.htm>.
- Hirschi, M., S. I. Seneviratne, and C. Schär (2006), Seasonal variations in terrestrial water storage for major mid-latitude river basins, *Journal of Hydrometeorology*, *7* (1), 39-60.
- Kaspar, F. (2004), Development and uncertainty analysis of a global hydrological model, PhD thesis (in German), Kassel University Press, ISBN 3-89958-071-0, Kassel, Germany.
- Legates, D. R., and C. J. Willmott (1990), Mean seasonal and spatial variability in gauge-corrected, global precipitation, *International Journal of Climatology*, *10*, 111-127.
- Lehner, B., and P. Döll (2004), Development and validation of a global database of lakes, reservoirs and wetlands, *Journal of Hydrology*, *296*, 1-22.
- Maheu, C., A. Cazenave, and C.R. Mechoso (2003), Water level fluctuations in the Plata Basin (South America) from Topex/Poseidon Satellite Altimetry, *Geophys. Res. Lett.*, *30* (3), 1143, doi:10.1029/2002GL016033.
- Masuda, K., Y. Hashimoto, H. Matsuyama, and T. Oki (2001), Seasonal cycle of water storage in major river basins of the world, *Geophysical Research Letters*, *28*, 3215-3218.
- Matsuyama, H., and K. Masuda (1997), Estimates of continental-scale soil wetness and comparison with the soil moisture data of Mintz and Serafini, *Climate Dynamics*, *13*, 681-689.
- Milly, P.C.D., and A.B. Shmakin (2002), Global modeling of land water and energy balances. Part I: The Land Dynamics (LaD) Model, *Journal of Hydrometeorology*, *3* (3), 283-299.
- Mitchell, T.D., T.R. Carter, P.D. Jones, M. Hulme, and M. New (2004), A comprehensive set of high-resolution grids of monthly climate for Europe and the globe: the observed record (1901-2000) and 16 scenarios (2001-2100), Tyndall Working Paper 55, Tyndall Centre, UEA, Norwich, UK.
- New, M.G., M. Hulme, and P.D. Jones (2000), Representing 20th century space-time climate variability. II: development of 1901-96 monthly grids of terrestrial surface climate, *Journal of Climate*, *13*, 2217-2238.
- Ngo-Duc, T., K. Laval, J. Polcher, A. Lombard, and A. Cazenave (2005), Effects of land water storage on global mean sea level over the past half century, *Geophys. Res. Lett.*, *32*, doi:10.1029/2005GL022719.
- Oki, T., K. Musiake, H. Matsuyama, and K. Masuda, Global soil moisture extraction using 4DDA and observational runoff data by combined atmospheric-river basin water balance (1995), *Second International Symposium on Assimilation of Observations in Meteorology and Oceanography*, WMO/TD, 651, 355-360, Tokyo, Japan.
- Priestley, C.H.B., and R.J. Taylor (1972), On the assessment of surface heat flux and evaporation using large-scale parameters, *Mon. Weather Rev.*, *100*, 81-92.
- Ramillien, G., F. Frappart, A. Cazenave, and A. Güntner (2005), Time variation of land water storage from an inversion of 2 years of GRACE geoids, *Earth and Planetary Science Letters*, *235*, 283-301, doi:10.1016/j.epsl.2005.1004.1005.
- Robock, A., C.A. Schlosser, K.Y. Vinnikov, N.A. Speranskaya, J.K. Entin, and S. Qiu (1998), Evaluation of the AMIP soil moisture simulations, *Global and Planetary Change*, *19* (1-4), 181-208.

- Robock, A., K.Y. Vinnikov, G. Srinivasan, J.K. Entin, S.E. Holinger, N.A. Speranskaya, S. Liu, and A. Namkhai (2000), The global soil moisture data bank, *Bull. Am. Meteorol. Soc.*, 81 (6), 1281-1299.
- Rodell, M., and J.S. Famiglietti (1999), Detectability of variations in continental water storage from satellite observations of the time dependent gravity field, *Water Resources Research*, 35 (9), 2705-2723.
- Rodell, M., and J.S. Famiglietti (2001), An analysis of terrestrial water storage variations in Illinois with implications for the gravity recovery and climate experiment (GRACE), *Water Resources Research*, 37 (5), 1327-1339.
- Rodell, M., P.R. Houser, U. Jambor, J. Gottschalck, K. Mitchell, C.-J. Meng, K. Arsenault, B. Cosgrove, J. Radakovich, M. Bosilovich, J.K. Entin, J.P. Walker, D. Lohmann, and D. Toll (2004), The Global Land Data Assimilation System, *Bull. Am. Meteorol. Soc.*, 85 (3), 381-394.
- Ropelewski, C.F., and M.S. Halpert (1987), North American precipitation and temperature patterns associated with the El Niño/ Southern Oscillation (ENSO), *Mon. Wea. Rev.*, 114, 2352-2362.
- Schmidt, R., P. Schwintzer, F. Flechtner, C. Reigber, A. Güntner, P. Döll, G. Ramillien, A. Cazenave, S. Petrovic, H. Jochmann, and J. Wunsch (2006), GRACE observations of changes in continental water storage, *Global and Planetary Change*, 18, doi: 10.1016/j.gloplacha.2004.1011.1018.
- Seneviratne, S.I., P. Viterbo, D. Lüthi, and C. Schär (2004), Inferring changes in terrestrial water storage using ERA-40 reanalysis data: The Mississippi River basin, *Journal of Climate*, 17, 2039-2057.
- Seo, K.-W., and C. R. Wilson (2005), Simulated estimation of hydrological loads from GRACE, *Journal of Geodesy*, DOI 10.1007/s00190-004-0410-5.
- Stuck, J., A. Güntner, and B. Merz (2006), ENSO impact on simulated South American hydro-climatology, *Advances in Geosciences*, 6, 227-236.
- Swenson, S., J. Wahr, and P.C.D. Milly (2003), Estimated accuracies of regional water storage variations inferred from the Gravity Recovery and Climate Experiment (GRACE), *Water Resources Research*, 39 (8), 1223, doi:10.1029/2002WR001808.
- Tapley, B. D., S. V. Bettadpur, M. Watkins, and C. Reigber (2004a), The gravity recovery and climate experiment: Mission overview and early results, *Geophysical Research Letters*, 31, L09607, doi:09610.01029/02004GL019920.
- Tapley, B.D., S.V. Bettadpur, J.C. Ries, P.F. Thompson, and M.M. Watkins (2004b), GRACE measurements of mass variability in the Earth system, *Science*, 305, 503-505.
- Vörösmarty, C.J., C.A. Federer, and A.L. Schloss (1998), Potential evaporation functions compared on US watersheds: Possible implications for global-scale water balance and terrestrial ecosystem modeling, *Journal of Hydrology*, 207, 147-169.
- Vörösmarty, C.J., P. Green, J. Salisbury, and R.B. Lammers (2000), Global water resources: Vulnerability from climate change and population growth, *Science*, 289 (5477), 284-288.
- Wagner, W., K. Scipal, C. Pathe, D. Gerten, W. Lucht, and B. Rudolf (2003), Evaluation of the agreement between first global remotely sensed soil moisture data with model and precipitation data, *Journal of Geophysical Research*, 108 (D19), 4611, doi:10.1029/2003JD003663.
- Wahr, J., M. Molenaar, and F. Bryan (1998), Time variability of the Earth's gravity field: Hydrological and oceanic effects and their possible detection using GRACE, *Journal of Geophysical Research*, 103 (12), 30205-30229.
- Wahr, J., S. Swenson, V. Zlotnicki, and I. Velicogna (2004), Time-variable gravity from GRACE: First results, *Geophysical Research Letters*, 31, L11501, doi:10.1029/2004GL019779.

Figure captions

Figure 1. Scheme of the water storage compartments and their interactions in the WGHM model (from Döll et al., 2003).

Figure 2. Major global Koeppen climate zones and sub-types after FAO [1997] (see Table 1 for an explanation of climate zone acronyms)

Figure 3. Mean annual continental water storage from WGHM, period 1961-1995

Figure 4. Mean seasonal total water storage change between months with maximum and minimum storage volume

Figure 5. Annual cycle of precipitation and water storage components for large river basins, mean monthly values for period 1961-1995.

Figure 6. Months with (a) minimum and (b) maximum total water storage based on mean annual cycle for 1961-1995.

Figure 7. (a) Time-space variations of total water storage (1.EOF) in South-America after removal of the mean seasonal variations, contours are mm water equivalent, (b) amplitude of the 1.EOF (black) and the NINO3 index (blue, top of figure) and wavelet power spectrum of the amplitude with level of 5% significance (black solid), contours are multiple of the amplitude variance.

Figure 8. Same as Figure 7, but for Australia.

Figure 9. Same as Figure 7, but for Europe. The blue curve in top of figure 9b represents the wintermean (January, February and March) of the NAO index from the Climate Prediction Center (CPC).

Figure 10. Time series of (a) precipitation on continents (CRU data), and (b) total continental water storage (simulated with WGHM and ORCHIDEE (*Ngo-Duc et al.* 2005)) and water storage of single storage components (simulated with WGHM). Annual anomalies relative to mean for the period 1961-1995.

Figure 11. Spatial autocorrelograms of monthly fields of (a) the sum of groundwater, soil water and snow storage, (b) total water storage including surface water; for the major Koeppen climate zones on the Northern hemisphere, based on simulation results of WGHM for 1961-1980

Figure 12. Seasonal variation of correlation lengths for monthly water storage fields (sum of groundwater, soil water, snow) for the major Koeppen climate zones on the Northern hemisphere

Tables

Table 1. Mean annual water storage characteristics for the Koeppen climate zones and sub-types (1961-1995)

Koeppen Climate Zone	Area	f_{sw}	P	AET	S_{smax}	S_{rmax}	TWS	Contribution of storage component to TWS						
	10^6 km^2	%	mm	mm	mm	mm	mm	<i>snow</i>	<i>soil</i>	<i>gw</i>	<i>lake</i>	<i>wetl</i>	<i>river</i>	<i>sw</i>
A, tropical	26.5	10.4	1859	1130	311	240	337	0	25	24	6	37	8	51
Af, no dry season	5.9	13.0	2806	1515	593	270	607	0	32	23	2	36	7	45
Am, short dry season	4.2	8.6	2294	1282	374	189	426	0	26	25	5	32	12	49
Aw, distinct dry season	16.4	9.9	1408	953	194	242	217	0	18	25	11	39	7	57
B, dry	41.5	4.4	270	217	76	99	30	4	19	20	20	32	5	57
BS, steppe	17.6	5.4	441	362	124	127	51	6	21	19	23	28	4	55
BW, desert	23.9	3.7	144	111	41	79	14	0	14	21	14	43	7	64
C, temperate	21.5	5.4	1146	689	189	134	180	1	27	24	14	28	6	48
Cf, no dry season	8.6	6.6	1364	776	226	171	266	1	29	23	17	24	6	47
Cw, dry winter	7.4	5.1	1203	740	169	114	143	0	20	26	8	39	6	54
Cs, dry summer	3.4	3.6	616	385	148	94	77	1	36	28	21	12	3	36
D, cold	29.1	13.4	561	324	288	382	258	17	15	9	32	25	2	59
Df, no dry season	4.6	19.7	948	447	274	616	478	16	13	10	37	23	1	61
Dw, dry winter	6.5	5.1	478	313	250	151	125	18	20	9	24	24	4	53
E, polar	11.7	8.3	452	236	143	246	160	46	11	5	24	13	1	37
ET, tundra	10.7	8.0	460	237	150	245	148	39	13	6	28	14	1	43
EF, arctic	1.1	11.1	375	222	81	254	278	87	3	2	3	5	0	8
Global	130.3	8.1	818	506	196	210	179	10	21	17	18	29	5	52

f_{sw} : areal fraction of surface water bodies (lakes, reservoirs, wetlands) on total area; P : precipitation (WGHM model input); AET : actual evapotranspiration (WGHM model output); S_{smax} : Water storage capacity in the soil zone (see equation 3); S_{rmax} : Water storage capacity in lakes and wetlands (see equation 6); TWS : total water storage

storage components: - *snow*: snow storage
 - *soil*: soil moisture
 - *gw*: groundwater
 - *lake*: lakes and reservoirs
 - *wetl*: wetlands
 - *river*: rivers
 - *sw*: total surface water (sum of *lake*, *wetl*, *river*)

Table 2. Water storage characteristics for major river basins (1961-1995) (see Table 1 for further abbreviations)

River basin	Area <i>10³ km²</i>	<i>P</i> <i>mm</i>	<i>AET</i> <i>mm</i>	<i>TWS</i> <i>mm</i>	ΔTWS <i>mm</i> <i>monthly</i>	ΔTWS <i>mm</i> <i>seasonal</i>	ΔTWS <i>mm</i> <i>interannual</i>	seasonal storage change ΔSI of storage component				Contribution of storage component to ΔTWS seasonal			
								<i>snow</i> <i>mm</i>	<i>soil</i> <i>mm</i>	<i>gw</i> <i>mm</i>	<i>sw</i> <i>mm</i>	<i>snow</i> <i>%</i>	<i>soil</i> <i>%</i>	<i>gw</i> <i>%</i>	<i>sw</i> <i>%</i>
Amazon	5922	2117	1149	459	33	196	30	0	66	57	80	0	33	27	40
Congo	3693	1490	1050	289	15	74	18	0	32	31	28	0	28	38	35
Mississippi	3232	784	535	176	14	83	22	33	37	16	26	31	44	-1	27
Nile	2887	649	518	117	14	83	16	0	33	14	45	0	33	16	52
Paraná	2568	1211	873	265	18	110	28	0	33	45	42	0	26	39	35
Yenissei	2544	456	271	176	13	75	12	111	14	16	34	146	3	-19	-31
Ob	2497	465	273	265	17	105	20	121	23	37	23	113	9	-30	7
Lena	2461	377	228	112	10	55	11	82	11	4	40	146	5	-6	-46
Yangtze	1922	1000	564	178	13	79	18	1	16	27	44	0	15	31	55
Amur	1874	554	363	145	10	58	15	36	18	28	30	7	26	30	37
Niger	1789	775	589	110	17	103	13	0	39	39	46	0	23	37	40
Mackenzie	1702	396	227	274	21	124	17	115	16	22	29	93	3	-16	20
Ganges/Brahmaputra	1571	1281	554	278	36	218	19	6	48	48	141	-2	18	21	64
Volga	1393	585	396	270	32	191	27	166	75	37	52	75	29	-5	1
Zambezi	1382	910	710	122	23	139	31	0	55	42	69	0	29	30	42
Nelson	1170	509	295	409	21	126	29	93	19	37	61	71	8	-23	45
Murray-Darling	1057	501	456	37	7	34	13	0	23	7	9	0	66	15	19
Saint-Lawrence	1048	827	384	828	39	231	46	178	43	46	94	73	15	-13	25
Amudarya/Syrdarya	1038	295	201	51	12	72	15	50	14	9	18	64	17	6	12
Orinoco	959	2319	1010	450	47	284	30	0	91	73	133	0	30	23	47
Oranje	952	338	301	16	3	17	6	0	10	5	6	0	50	22	28
Tocantins	876	1816	1071	470	53	316	36	0	64	111	149	0	19	35	46
Euphrates	869	309	211	57	11	69	13	19	20	12	35	24	25	14	38
Indus	836	460	282	67	11	44	14	29	11	10	23	35	20	10	35
Yukon	831	264	163	136	11	66	15	64	9	5	15	94	4	-6	8
Danube	796	776	482	169	25	149	28	79	73	25	23	45	46	4	5
Mekong	792	1492	893	251	35	210	18	0	68	70	84	0	30	32	39
Huanghe	758	435	353	53	7	42	11	1	19	17	11	0	39	37	23
Okavango	704	519	457	44	8	51	16	0	29	21	15	0	44	38	18
Columbia	668	627	299	201	34	206	33	162	44	18	38	77	19	1	3

Table 3 Monthly and seasonal variations of total water storage (ΔTWS) and contributions of individual storage components for the major Koeppen climate zones and sub-types (1961-1995) (see also Table 1 for further abbreviations).

Koeppen Climate Zone	ΔTWS , monthly	ΔTWS , seasonal	Contribution of storage component to ΔTWS seasonal						
	<i>mm</i>	<i>mm</i>	<i>snow</i>	<i>soil</i>	<i>Gw</i>	<i>lake</i>	<i>wetl</i>	<i>river</i>	<i>sw</i>
			%	%	%	%	%	%	%
A, tropical	42	241	0	37	28	4	17	15	36
Af, no dry season	48	270	0	47	23	1	11	18	30
Am, short dry season	57	327	0	40	27	1	8	24	33
Aw, distinct dry season	36	209	0	32	30	5	21	12	38
B, dry	7	42	9	27	16	8	26	15	49
BS, steppe	12	67	14	36	17	10	17	9	36
BW, desert	4	24	6	20	15	6	33	20	59
C, temperate	28	159	4	44	24	5	11	11	27
Cf, no dry season	33	186	7	46	21	4	10	12	26
Cw, dry winter	28	162	0	36	29	4	17	14	35
Cs, dry summer	19	114	6	54	22	8	6	4	18
D, cold	27	160	68	18	-4	3	9	7	19
Df, no dry season	45	270	82	21	-9	2	7	1	10
Dw, dry winter	15	90	48	21	8	5	7	11	22
E, polar	23	138	86	9	0	-1	4	1	5
ET, tundra	24	143	87	10	-1	-1	4	1	4
EF, arctic	15	91	75	8	6	2	9	1	12
Global	23	137	26	28	14	4	16	11	32

Table 4 Seasonal storage variation of individual storage components for the major Koeppen climate zones (1961-1995) (in mm).

Koeppen Climate Zone	<i>Snow</i>		<i>soil water</i>		<i>groundwater</i>		<i>surface water</i>	
	$\Delta S1$	$\Delta S2$	$\Delta S1$	$\Delta S2$	$\Delta S1$	$\Delta S2$	$\Delta S1$	$\Delta S2$
A, tropical	0	0	99	90	76	67	89	84
B, dry	6	4	15	13	10	7	20	18
C, temperate	8	6	75	69	47	39	48	45
D, cold	130	113	47	29	32	-10	56	28
E, polar	124	119	22	13	13	0	29	5
Global	43	39	50	42	35	20	47	37

$\Delta S1$: seasonal storage variation of a storage component computed as the difference between maximum and minimum monthly storage of the mean annual cycle;

$\Delta S2$: seasonal storage variation of a storage component computed as the difference between the months at which the monthly storage of the mean annual cycle of TWS is at its maximum and minimum.

Table 5 Interannual variations of total water storage (ΔTWS) and contributions of individual storage components for the major Koeppen climate zones and sub-types (1961-1995) (see also Table 1 for further abbreviations).

Koeppen Climate Zone	ΔTWS	Contribution of storage component to ΔTWS interann						
	interann	snow	soil	Gw	lake	wetl	river	sw
	mm	%	%	%	%	%	%	%
A, tropical	50	0	32	28	6	21	13	39
Af, no dry season	75	0	46	26	1	12	15	28
Am, short dry season	56	0	38	28	2	9	22	33
Aw, distinct dry season	40	0	25	29	8	26	10	45
B, dry	12	6	22	23	9	33	8	51
BS, steppe	18	8	29	25	12	21	6	39
BW, desert	7	4	17	21	6	43	10	59
C, temperate	39	3	36	31	6	15	9	30
Cf, no dry season	54	4	36	29	6	14	10	30
Cw, dry winter	29	0	33	33	5	19	11	35
Cs, dry sommer	24	6	39	33	10	9	4	22
D, cold	37	33	27	12	11	13	4	28
Df, no dry season	58	37	21	15	15	11	2	27
Dw, dry winter	23	29	36	12	8	10	5	23
E, polar	27	56	18	7	10	8	2	20
ET, tundra	27	54	19	7	11	8	2	20
EF, artic	31	67	10	6	5	11	1	17
Global	31	16	27	21	9	20	7	36

Table 6. Spatial correlation lengths (km) of water storage (sum of groundwater, soil water and snow, (GSS), or total water storage including surface water, (TWS)) and monthly storage change (ΔGSS , ΔTWS). Minimum mean, and maximum values for monthly fields simulated with WGHM for the period 1961-95.

	GSS			TWS			ΔGSS	ΔTWS
	min	mean	max	min	mean	max	mean	mean
Climate A (tropical)	520	910	1230	130	170	180	450	220
Climate B (dry)	560	830	1340	90	100	120	600	150
Climate C (temperate)	360	790	1380	150	160	180	890	470
Climate D (cold)	650	750	970	80	90	92	720	170
Climate E (polar)	230	390	530	110	140	180	470	230

Table 7. Sensitivity of WGHM simulation results in terms of seasonal water storage change ($\Delta TWS_{seasonal}$) to parameter and input data uncertainties. X denotes river basins with a high parameter sensitivity ($|r_{spear}| > 0.2$) for at least one parameter in a certain process category (columns 1-6), with high sensitivity to the tuning parameter γ (column 7), to uncertainty of precipitation (column 8), or air temperature (column 9). Column 10 is $\Delta TWS_{seasonal}$ from Table 2, Column 11 the standard deviation of $\Delta TWS_{seasonal}$ for the 2000 Monte-Carlo runs.

Basin	1 <i>Radiation/ Evaporation demand</i>	2 <i>Inter- ception</i>	3 <i>Snow</i>	4 <i>Soil water</i>	5 <i>Ground water</i>	6 <i>Surface water</i>	7 <i>Tuning parameter γ</i>	8 <i>Precip</i>	9 <i>Temp</i>	10 <i>$\Delta TWS_{seasonal}$</i>	11 <i>$\sigma(\Delta TWS_{seasonal})$</i>
										<i>mm</i>	<i>mm</i>
Amazon	X					X				196	47
Congo	X			X		X				74	21
Mississippi			X	X			X	X		83	14
Nile	X			X		X		X		83	13
Paraná	X			X		X				110	21
Yenisei			X				X	X		75	15
Ob							X	X		105	22
Lena			X			X				55	13
Yangtze	X			X		X				79	15
Amur							X	X		58	5
Niger	X			X		X		X		103	17
Mackenzie	X						X	X		124	8
Ganges/Brahmaputra				X		X	X	X		218	34
Volga			X				X	X		191	32
Zambeze	X			X			X			139	29
Nelson	X					X	X			126	11
Saint-Lawrence	X		X			X	X	X		231	24
Oranje	X	X		X		X	X			17	5
Tocantins	X			X		X				316	54
Indus			X	X		X		X		44	5
Yukon	X		X					X	X	66	5
Danube			X	X			X	X	X	149	20

Table 8. Mean seasonal water storage change for large river basins, simulated with WGHM and derived from three combined atmospheric-terrestrial water balance studies.

Data source	<i>WGHM</i>	<i>Oki</i>	<i>Hirschi</i>	<i>Masuda</i>
Period	1961-95	1989-92	~1958-2000	~1973-95
	<i>mm</i>	<i>mm</i>	<i>mm</i>	<i>mm</i>
Amazon	196	382		204
Congo	74	124		91
Mississippi	83	104	99	91
Nile	83			69
Paraná	110	60		101
Yenissei	75		104	121
Ob	105	140	143	123
Lena	55	140	107	106
Yangtze	79			99
Amur	58		43	43
Niger	103			90
Mackenzie	124	114	96	93
Ganges/Brahmaputra	218	324		237/229
Volga	191	182	158	147
Zambeze	139			155
Nelson	126			59
Murray-Darling	34	86	58	19
Saint-Lawrence	231			103
Amudarya/Syrdarya	72		246/182	202/121
Orinoco	284			284
Oranje	17	178		22
Tocantins	316			234
Euphrates	69			120
Indus	44			106
Yukon	66		116	121
Danube	149		131	143
Mekong	210			209
Huanghe	42	86		64
Okavango	51			
Columbia	206	292	269	282

Figures

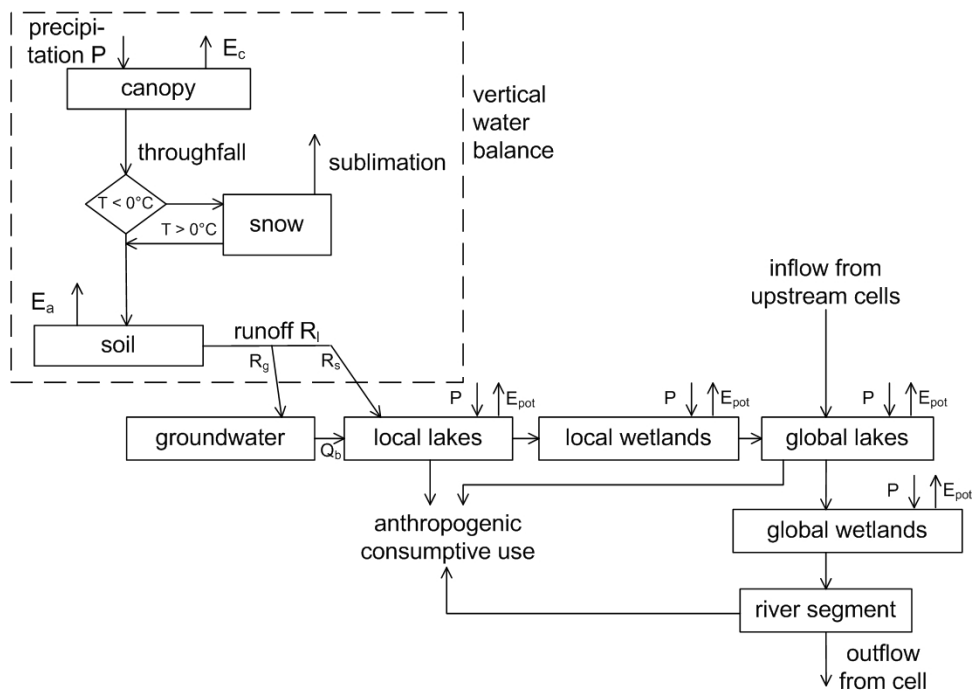


Figure 1. Scheme of the water storage compartments and their interactions in the WGHM model (modified after Döll et al., 2003).

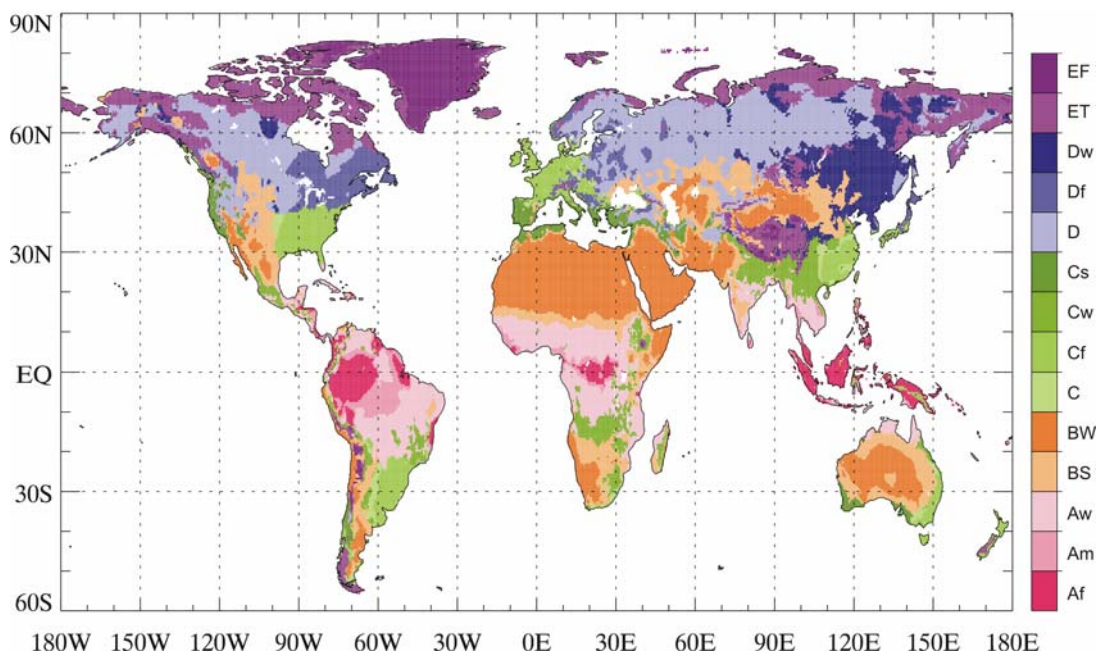


Figure 2. Major global Koeppen climate zones and sub-types after FAO [1997] (see Table 1 for an explanation of climate zone acronyms)

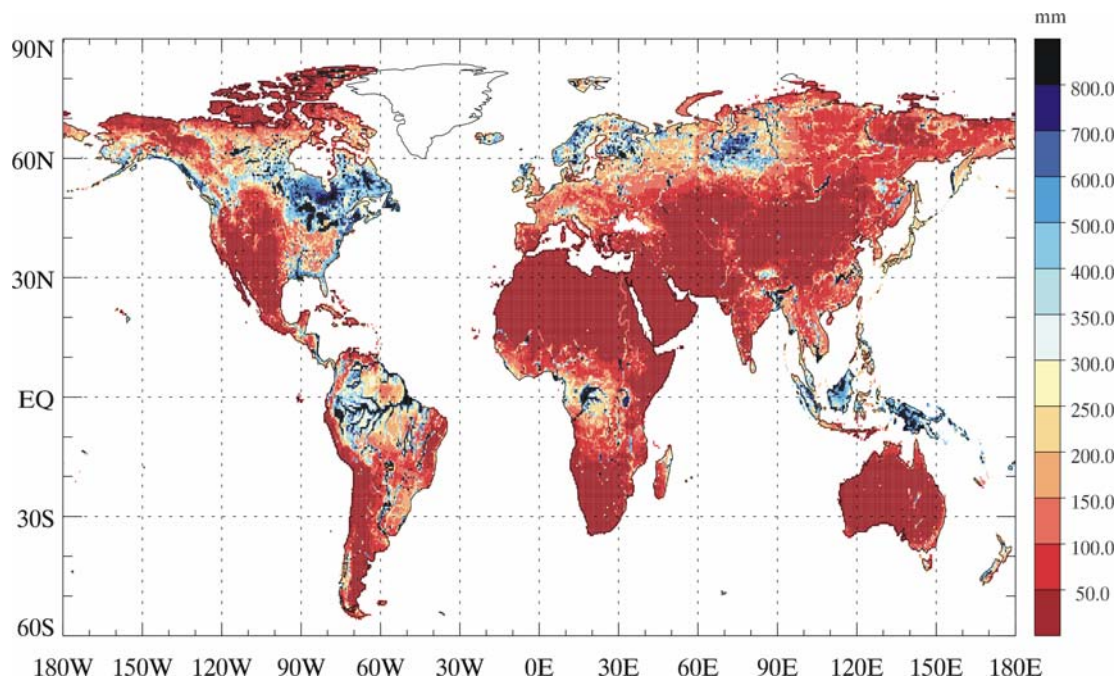


Figure 3. Mean annual continental water storage from WGHM, period 1961-1995

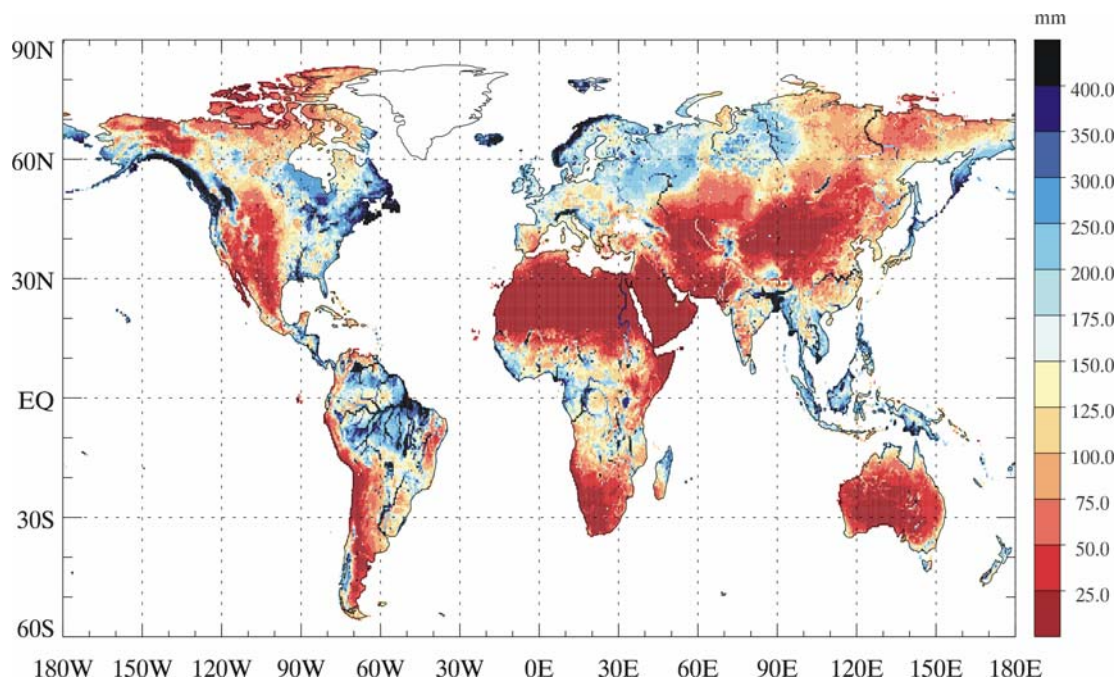


Figure 4. Mean seasonal total water storage change between months with maximum and minimum storage volume

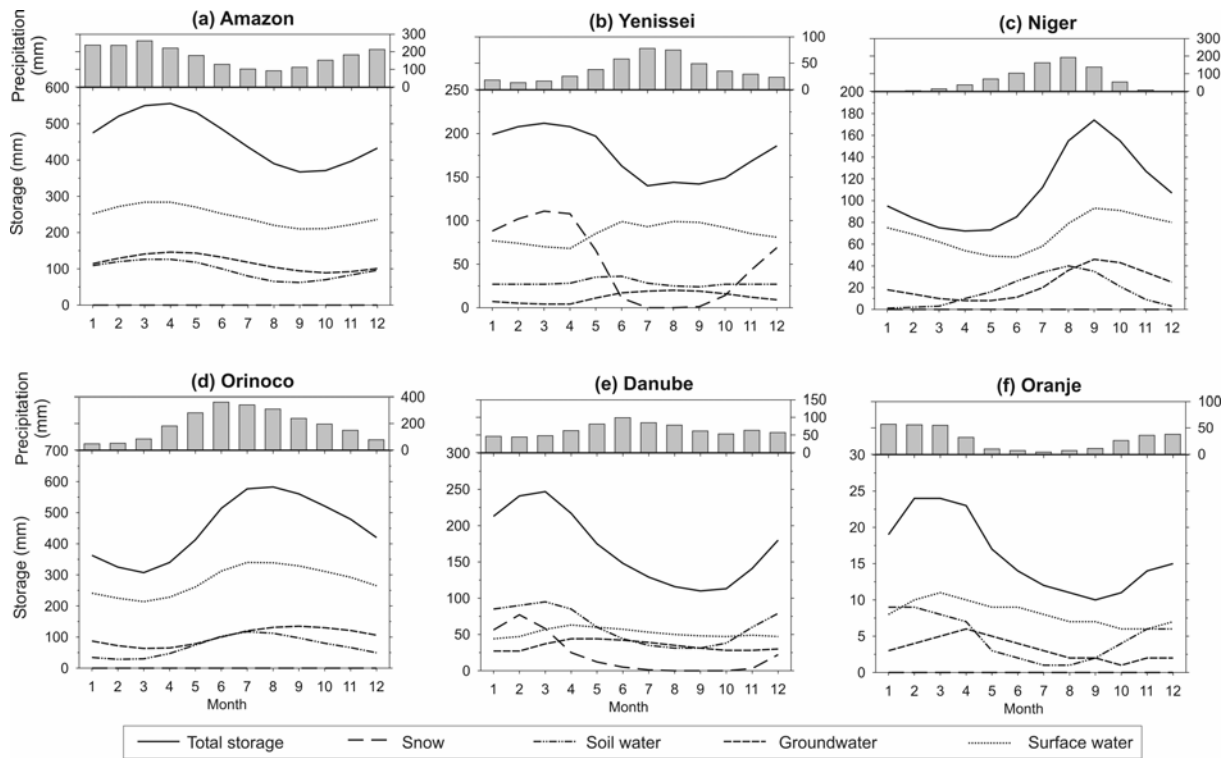


Figure 5. Annual cycle of precipitation and water storage components for large river basins, mean monthly values for period 1961-1995.

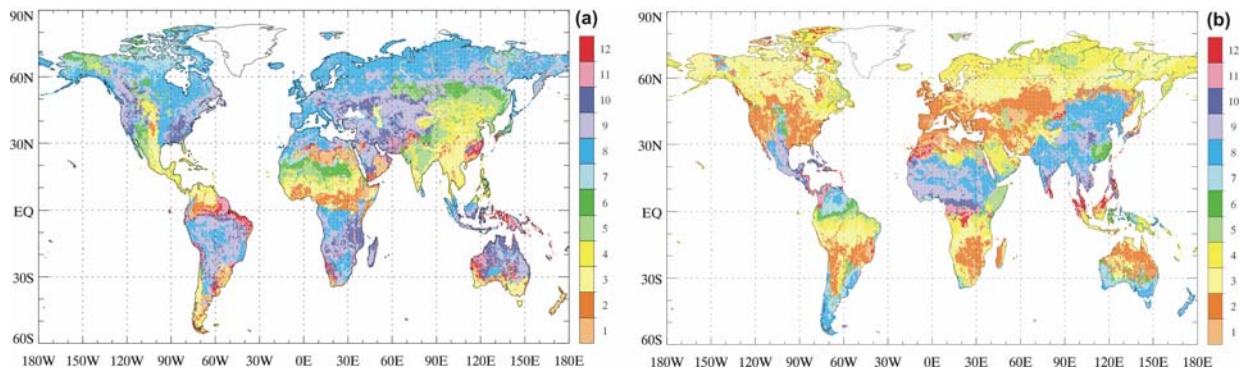


Figure 6. Months with (a) minimum and (b) maximum total water storage based on mean annual cycle for 1961-1995.

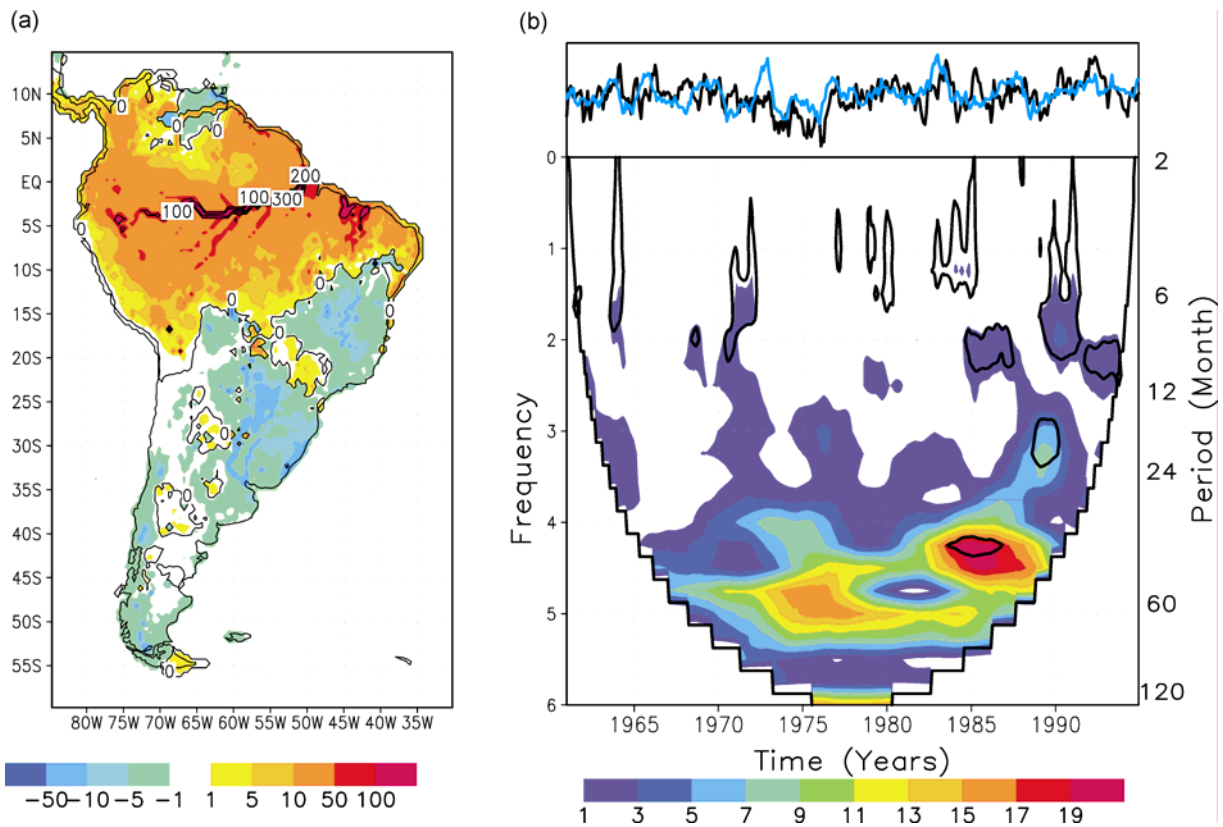


Figure 7. (a) Time-space variations of total water storage (1.EOF) in South-America after removal of the mean seasonal variations, contours are mm water equivalent, (b) amplitude of the 1.EOF (black) and the NINO3 index (blue, top of figure) and wavelet power spectrum of the amplitude with level of 5% significance (black solid), contours are multiple of the amplitude variance.

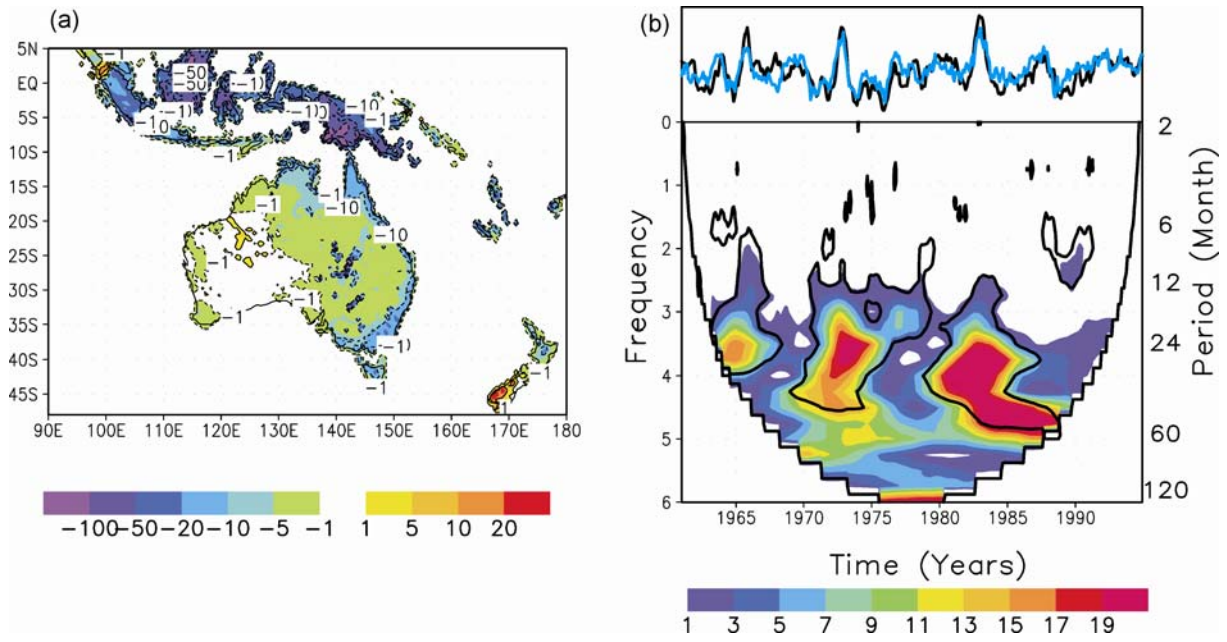


Figure 8. Same as Figure 7, but for Australia.

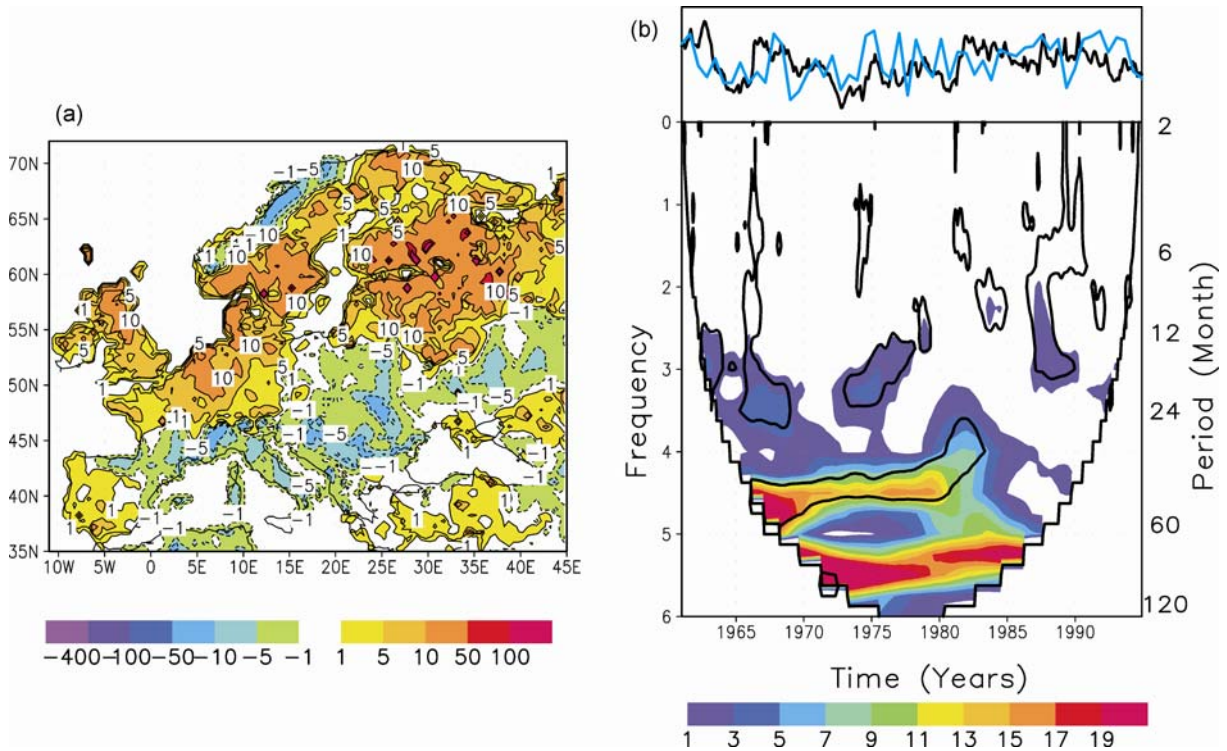


Figure 9. Same as Figure 7, but for Europe. The blue curve in top of figure 9b represents the wintermean (January, February and March) of the NAO index from the Climate Prediction Center (CPC).

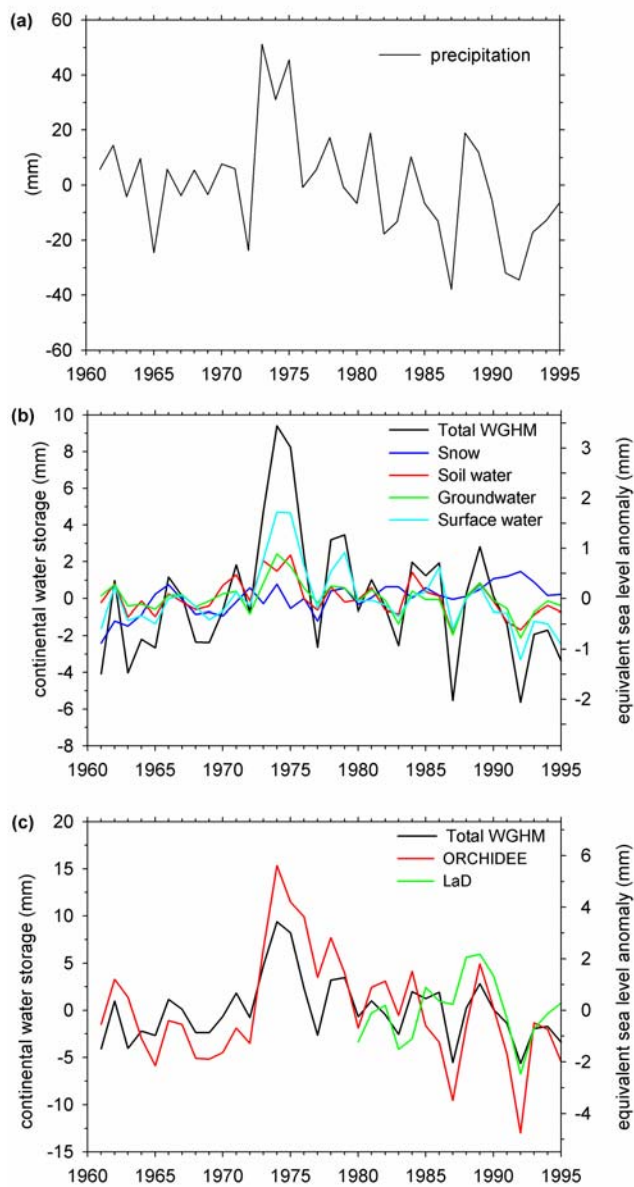


Figure 10. Time series of (a) precipitation on continents (CRU data), (b) continental water storage (total and single compartments simulated with WGHM), (c) continental water storage from WGHM, ORCHIDEE [Ngo-Duc et al. 2005] and LaD [Milly and Shmakin, 2002]. Annual anomalies relative to mean for the period 1961-1995 (1980-1995 for LaD), in (b) and (c) also expressed as equivalent global seal level anomaly..

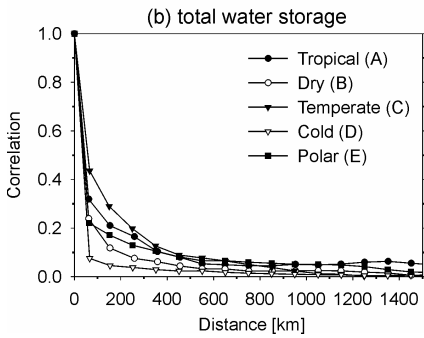
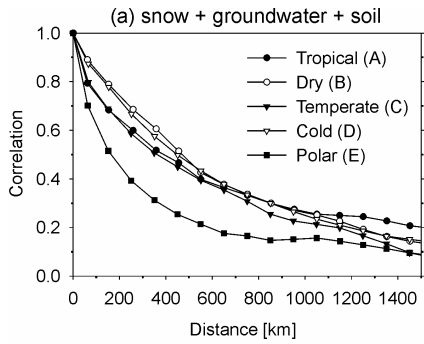


Figure 11. Spatial autocorrelograms of monthly fields of (a) the sum of groundwater, soil water and snow storage, (b) total water storage including surface water; for the major Koeppen climate zones on the Northern hemisphere, based on simulation results of WGHM for 1961-1980

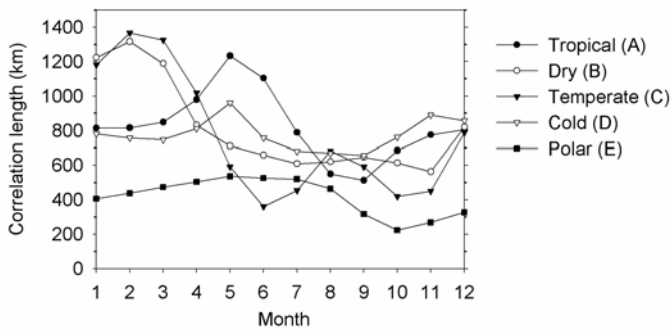


Figure 12. Seasonal variation of correlation lengths for monthly water storage fields (sum of groundwater, soil water, snow) for the major Koeppen climate zones on the Northern hemisphere